

OPTIMUM DESIGN OF FREE STANDING CANTILEVER RETAINING WALLS

A Thesis Submitted
in Partial Fulfilment of the Requirements
for the Degree of

MASTER OF TECHNOLOGY

by

MANOJ S MEDHEKAR

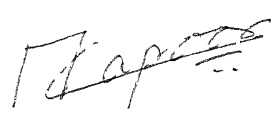
to the

DEPARTMENT OF CIVIL ENGINEERING
INDIAN INSTITUTE OF TECHNOLOGY KANPUR

APRIL, 1990

CERTIFICATE

It is certified that the work contained in the thesis entitled " OPTIMUM DESIGN OF FREE STANDING CANTILEVER RETAINING WALLS " by Manoj S. Medhekar, has been carried out under my supervision and that this work has not been submitted elsewhere for a degree.


(M P. KAPOOR)

Professor

Department of Civil Engineering

Indian Institute of Technology

Kanpur

April, 1990

-1 0181

CENTRAL LIBRARY

1110025

CE-1990-M-MED-CPY

ABSTRACT

The optimum design of a free standing cantilever retaining wall has been carried out in this work

The analysis of the wall has been carried out assuming that the foundation is, (i) Rigid and (ii) Flexible For rigid foundation behavior, a linear bearing pressure distribution is obtained under the wall footing, which simplifies the analysis considerably. For flexible foundation behavior, the wall footing has been modeled as a beam on a one parameter elastic foundation, subject to loads caused by the retained earth. This analysis is carried out by the variational finite element method.

The objective function to be minimized is the material cost of the retaining wall, per meter length. Constraints are considered for stability of the soil, the retaining wall, and for the structural strength requirements of the wall.

The resulting non-linear optimum design problem is solved by the interior penalty function method The Davidon-Fletcher-Powell variable metric method is used to carry out unconstrained minimization. A three point quadratic interpolation method is used to perform linear minimization

Results are presented for four classes of cohesionless soil with the wall heights varying from three to six meters

ACKNOWLEDGEMENT

I take this opportunity to thank Dr M P Kapoor for his guidance and encouragement during the course of this work.

I am grateful to Dr. S K. Jain for permitting me to use all the facilities at his disposal

I am very much thankful to my friends, Sameer, Gehad, Rajesh, Vivek, G K and Shankha for their help and co-operation at different stages of my work

I would like to thank Mr. Vajpayee and Mr. Verma for their adept draftsmanship

Manoj

TABLE OF CONTENTS

<u>Chapter</u>		<u>Page</u>
	LIST OF FIGURES	vii
	LIST OF TABLES	ix
	LIST OF SYMBOLS	x
I	INTRODUCTION	
	1 1 Introduction	1
	1 2 Scope of the Present Work	2
	1.3 Lateral Earth Pressure Phenomena	3
	1 3 1 Soil Properties	3
	1 3 2 Types of Lateral Earth Pressure	4
	1 3 3 Computation of Lateral Earth Pressure	5
	1 4 Forces Acting on Retaining Walls	7
	1 5 Brief Review of Literature	8
II	METHOD OF ANALYSIS	
	2.1 General	14
	2.1 Analysis of the Wall Stem	14
	2.3 Analysis of the Wall Footing	15
	2.3 1 Rigid Foundation Approach	15
	2.3.2 Flexible Foundation Approach	16
	2 4 Finite Element Analysis of a Beam on a Winkler Foundation	17
	2.5 Discretization	22
III	FORMULATION OF THE OPTIMUM DESIGN PROBLEM	
	3.1 Introduction	29
	3.2 Design Variables and Preassigned Parameters	29
	3.3 Constraints	30
	3.4 Side Constraints	35
	3.5 Objective Function	36
IV	METHOD FOR OPTIMUM DESIGN	
	4.1 General	41
	4.2 Interior Penalty Function Method	41
	4.3 Unconstrained Minimization	43
	4.4 Linear Minimization	44
	4.5 Initial Feasible Design	45

V	RESULTS, DISCUSSION AND CONCLUSIONS	
5.1	General	51
5.2	Soil: Gravel	52
5.3	Soil: Well Graded Sand	55
5.4	Soil: Uniformly Graded Sand	57
5.5	Soil: Non-Plastic Silt	59
5.6	Some Salient Observations	61
5.7	Guidelines for Preliminary Optimum Design	62
5.8	Conclusions	63
	LIST OF REFERENCES	70
	APPENDIX A: Meyerhof's Bearing Capacity Equations	72
	APPENDIX B: Computation of Factor of Safety for Slip Circle Failure	74

LIST OF FIGURES

<u>Figure</u>		<u>Page</u>
1.1	PARTS OF A RETAINING WALL	9
1.2	TYPES OF RETAINING WALLS	10
1.3	TYPES OF CANTILEVER WALL	11
1.4	RANKINE EARTH PRESSURE THEORY	12
1.5	FORCES ACTING ON A RETAINING WALL	13
2.1	FORCES ACTING ON THE WALL STEM	24
2.2	DESIGN LOADING ON THE TOE AND HEEL PROJECTIONS	25
2.2(a)	RESULTANT LOADING ON THE TOE PROJECTION	25
2.2(b)	RESULTANT LOADING ON THE HEEL PROJECTION	25
2.3	DIFFERENTIAL EQUATION OF A BEAM ON A WINKLER FOUNDATION	26
2.4	A TYPICAL BEAM ELEMENT	27
2.5	DISCRETIZATION AND LOADING ON FOOTING	28
3.1	DESIGN VARIABLES	39
3.2	STABILITY AGAINST SLIP CIRCLE FAILURE	40
4.1	FLOWCHART FOR INTERIOR PENALTY FUNCTION METHOD	46
4.2	FLOWCHART FOR DAVIDON - FLETCHER - POWELL METHOD	47
4.3	FLOWCHART FOR QUADRATIC INTERPOLATION	48
4.4	INITIAL FEASIBLE DESIGN	50
5.1(a)	VARIATION OF MINIMUM COST WITH RESPECT	64
to	TO HEIGHT OF WALL	
5.1(d)		
5.2	VARIATION OF SIZING VARIABLES WITH HEIGHT OF WALL FOR SOIL GRAVEL	65
5.3	TYPICAL VARIATION OF BEARING PRESSURE FOR FLEXIBLE FOUNDATION	66

5 4	VARIATION OF SIZING VARIABLES WITH HEIGHT OF WALL FOR SOIL WELL GRADED SAND	67
5 5	VARIATION OF SIZING VARIABLES WITH HEIGHT OF WALL FOR SOIL UNIFORMLY GRADED SAND	68
5.6	VARIATION OF SIZING VARIABLES WITH HEIGHT OF WALL FOR SOIL NON-PLASTIC SILT	69
B.1	FACTOR OF SAFETY FOR SLIP CIRCLE FAILURE	77

LIST OF TABLES

<u>Table</u>		<u>Page</u>
1.1	MOVEMENT OF THE WALL NECESSARY TO PRODUCE ACTIVE PRESSURE	6
5 1	REPRESENTATIVE PROPERTIES OF SOIL	51
5 2	VARIATION OF MINIMUM COST WITH HEIGHT OF WALL FOR SOIL: GRAVEL	52
5.3	VARIATION OF MINIMUM COST WITH HEIGHT OF WALL FOR SOIL: WELL GRADED SAND	55
5.4	VARIATION OF MINIMUM COST WITH HEIGHT OF WALL FOR SOIL: UNIFORMLY GRADED SAND	57
5.5	VARIATION OF MINIMUM COST WITH HEIGHT OF WALL FOR SOIL: NON-PLASTIC SILT	59
5 6	SIZING VARIABLES FOR NEAR OPTIMUM DESIGN	62

LIST OF SYMBOLS

All symbols are explained when they appear first in the text. Only those symbols which appear more than once are listed below.

ϕ, ϕ_b	-	Angle of shearing resistance of the soil
c, c_b	-	Cohesion of the soil
s	-	Shearing strength of the soil
γ	-	Density of the soil
K_s	-	Modulus of subgrade reaction
P_a	-	Resultant active earth pressure
K_a	-	Coefficient of active earth pressure
P_p	-	Resultant passive earth pressure
K_p	-	Coefficient of passive earth pressure
P_b	-	Earth pressure on the wall stem
W_{st}	-	Self weight of the stem
M_b	-	Bending moment at the base of the stem
P_{heel}	-	Foundation bearing pressure at the heel of the wall
P_{toe}	-	Foundation bearing pressure at the toe of the wall
B	-	Base width of the wall
e	-	Eccentricity of the resultant loading on the base
X	-	Design vector
$F(X)$	-	Objective function to be minimized
$g_j(X)$	-	j^{th} inequality constraint
N	-	Number of design variables
m	-	Total number of inequality constraints
H_w	-	Total height of the wall

CHAPTER 1

INTRODUCTION

1.1 Introduction

A wall designed to maintain a difference in the elevations of the ground surfaces on each side of the wall is called a retaining wall. It is a very common civil engineering structure and is used extensively in railways, bridges, canals and other engineering works. Fig 1.1 identifies the parts of and terms used in retaining wall design. Fig 1.2 illustrates the various types of retaining walls in use.

Retaining walls require substantial dead weight to resist overturning and sliding from lateral earth pressure. A gravity retaining wall utilizes entirely its own weight to produce the necessary stability. Cantilever and counterfort retaining walls utilize the weight of the soil itself to produce stability. Semi-gravity walls are intermediate between the cantilever and gravity types. Mechanically reinforced earth walls which use reinforcement in the backfill to resist the lateral earth pressure are also in use.

Amongst the reinforced concrete retaining walls, the cantilever wall is most widely used as it is economical. It is, therefore, intended to investigate and study the optimum design of cantilever retaining walls.

Cantilever retaining walls are used in basement of buildings, as abutments for bridges, as flood walls in irrigation works as well as for retaining ores, minerals and other granular materials.

While the cantilever retaining walls used in buildings and bridges are partially restrained at their free end, the others are free standing

Different types of free standing cantilever retaining walls are illustrated in Fig.1 3. These walls are seen to be made up of three cantilever beams; the vertical stem, the toe projection and the heel projection. Fillets may be provided when the depth of the heel and toe projections are unequal. The sliding resistance can be increased by providing a key.

1 2 Scope of the Present Work

The present work deals with the optimum design of a free standing cantilever retaining wall as shown in Fig.1.3(c).

The analysis of the wall footing has been carried out by (i) conventional method and (ii) finite element method. The conventional method is the one which is used even now in most of the design offices. It assumes the foundation as rigid, whereby, a linear bearing pressure distribution is obtained under the wall footing. This considerably simplifies the analysis. The second method used in the present work is a more rigorous and realistic approach as it considers soil structure interaction. The wall footing has been modeled as a beam on a one parameter elastic foundation, subject to loads caused by the retained earth. The variational finite element method has been used to carry out this analysis. Both these methods of analysis are presented in chapter two.

The objective function for optimum design is to minimize the material cost of the retaining wall per meter length. Constraints

arise due to the requirements of stability of the soil containing the wall, stability of the wall itself, and the structural strength requirements of the wall. The formulation of the optimum design problem is discussed in chapter three.

The resulting inequality constrained nonlinear mathematical programming problem is solved by the interior penalty function method. The Davidon - Fletcher - Powell variable metric algorithm has been used for unconstrained minimization. A three point quadratic interpolation method has been used for linear minimization. These methods are discussed in chapter four.

Results are presented in chapter five for four classes of cohesionless soils, namely, gravel, well graded sand, uniformly graded sand and non-plastic silt.

1.3 Lateral Earth Pressure Phenomena

This section discusses the relevant soil properties, types of lateral earth pressure and the computation of lateral earth pressure

1.3.1 Soil Properties

The important soil properties used in the present work are defined below.

With reference to the direct shear test (Huntington, 1957), we define

- (a) Angle of shearing resistance (ϕ) as the slope of the rupture line.
- (b) Cohesion (c) as the unit strength of the material

corresponding to zero normal pressure on the surface of failure.

- (c) Shearing strength (s) expressed by the Coulomb's equation as

$$s = c + n \tan \phi \quad (1.1)$$

where s is the unit shearing strength of the soil,

n is the unit normal pressure on the surface of failure,

c and ϕ are as defined above.

Further, we define,

- (d) Density of the soil (γ) which varies with the moisture content and the degree of compaction of the soil

and

- (e) Modulus of subgrade reaction (K_s). Let the average contact pressure between the foundation and the soil be denoted by P_f . If the corresponding average settlement is denoted by Δ_f , then, the ratio

$$K_s = \frac{P_f}{\Delta_f} \quad (1.2)$$

is called the modulus of subgrade reaction.

1.3.2 Types of Lateral Earth Pressure

The lateral pressures in a soil mass are greatly affected by any lateral deformation which the mass may have experienced. Lateral earth pressures are classified as (i) earth pressure at rest (ii) active earth pressure and (iii) passive earth pressure.

Earth pressure at rest is associated with zero horizontal strain in the soil mass. This takes place in natural deposits.

Active earth pressure exists in a soil mass when it has been extended laterally. This is the minimum pressure that the soil can exert on the wall.

Passive earth pressure exists in a soil mass when it has been compressed laterally. This is the maximum pressure that the soil can exert on the wall.

The magnitude of the active and passive pressures depend on the shearing strength, s , of the soil.

1.3.3 Computation of Lateral Earth Pressure

All theories and methods for determining lateral earth pressure due to cohesionless or cohesive soil can be grouped under Rankine's or Coulomb's method according to their basic assumptions. As suggested by Huntington (1957), Rankine's method can be used for free standing cantilever retaining walls without significant error. Hence, in the present work, Rankine's method has been used to evaluate the lateral earth pressures.

Rankine's equations give the lateral earth pressure on the virtual back of the wall. Referring to Fig.1.4, the resultant active earth pressure is given by

$$P_a = \frac{K_a \gamma H^2}{2} \quad (1.3)$$

where $K_a = \cos \omega \left[\frac{\cos \omega - \sqrt{\cos^2 \omega - \cos^2 \phi}}{\cos \omega + \sqrt{\cos^2 \omega - \cos^2 \phi}} \right]$

ω is the inclination of the surcharge to the horizontal,

H is the height of the virtual back of the wall,

K_a is the coefficient of active earth pressure.

The resultant passive earth pressure is given by

$$P_p = \frac{K_p \gamma H^2}{2} \quad (14)$$

where $K_p = \cos \omega \left[\frac{\cos \omega + \sqrt{\cos^2 \omega - \cos^2 \phi}}{\cos \omega - \sqrt{\cos^2 \omega - \cos^2 \phi}} \right]$

K_p is the coefficient of passive earth pressure.

The Rankine earth pressure theory requires adequate lateral deformation in the soil to mobilize the maximum shearing strength of the soil. The amount of wall movement required to produce the active or passive states in the soil depends mainly on the type of backfill material used. Table 1.1 gives the outward movement of the wall which is necessary to produce an active state of stress in the retained soil.

TABLE 1.1. MOVEMENT OF WALL NECESSARY TO PRODUCE ACTIVE PRESSURE

Soil type	Wall yield
Cohesionless, dense	0.001 H - 0.002 H
Cohesionless, loose	0.002 H - 0.004 H
Cohesive, firm	0.01 H - 0.02 H
Cohesive, soft	0.02 H - 0.05 H

The wall deformation required to produce the active state in a cohesive backfill may be up to ten times greater than that for a cohesionless backfill. Also, cohesive soils have low shearing strengths. Thus, the corresponding active earth pressure for a particular wall movement will be higher if cohesive backfill is

used Hence, cohesive backfills are not considered in the present work

For free standing cantilever retaining walls with cohesionless backfills, on soil foundations, adequate movement usually takes place so that the active earth pressure obtained by Rankine's equations may be assumed to act on the wall

1.4 Forces Acting on Retaining Walls

The forces acting on a free standing cantilever wall are illustrated in Fig.1.5 A unit length of the cross section of the wall and the retained soil is considered for the purpose of analysis and design of the wall The various forces which act on the wall are as follows.

- (a) The weight of the wall, weight of the soil above the heel and the toe projections. The resultant of these weights is denoted by W .
- (b) The active earth pressure against the back of the wall, denoted by P_a . This is due to the lateral thrust of the retained earth It is calculated on the vertical plane through the rear of the heel which is referred to as the virtual back of the wall.
- (c) The normal component of the foundation pressure. The resultant of this is denoted by ΣV .
- (d) The horizontal component of foundation pressure. The resultant of these components is indicated by ΣH .
- (e) Passive earth pressure against the face of the wall, denoted by P_p .

The present work considers the forces (a) through (e). However, the following additional forces may arise depending on the situation and the purpose for which a wall is constructed:

- (f) Surcharge loads,
- (g) Water and seepage pressures,
- (h) Uplift,
- (i) Vibration due to traffic,
- (j) Impact,
- (k) Ice thrust and frost action,
- (l) Earthquake force in seismic zones

Forces from (f) to (l) listed above, have not been considered in the present work

1.5 Brief Review of Literature

Keskar (1976) carried out the optimum design of a cantilever retaining wall considering rigid foundation behavior only. The optimum design problem had four sizing variables and eight behavior and side constraints each. Results were presented for five classes of soil.

Hetenyi (1946) published classical solutions for a finite beam on an elastic foundation with various boundary conditions. Later, Wang (1970) and Bowles (1974) gave the finite element solution for finite beams on elastic foundation.

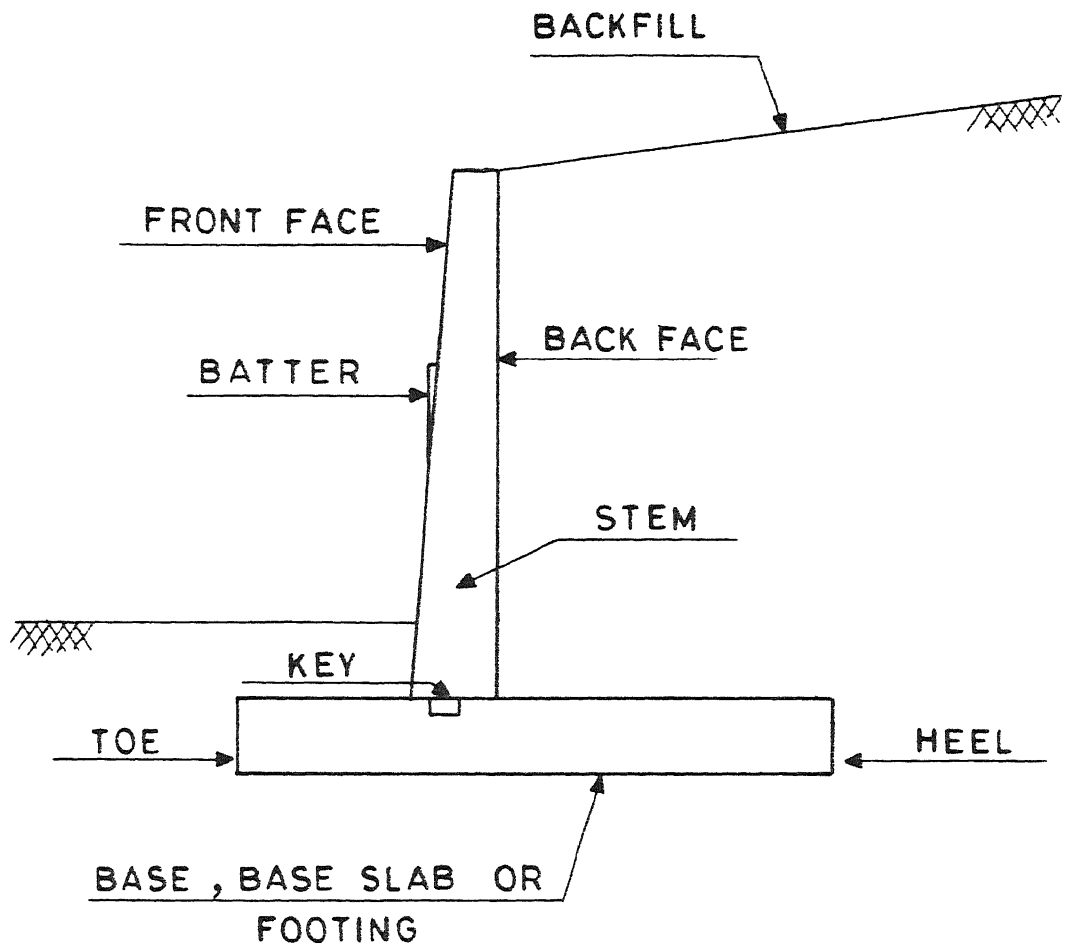


FIG.1.1: PARTS OF A RETAINING WALL .

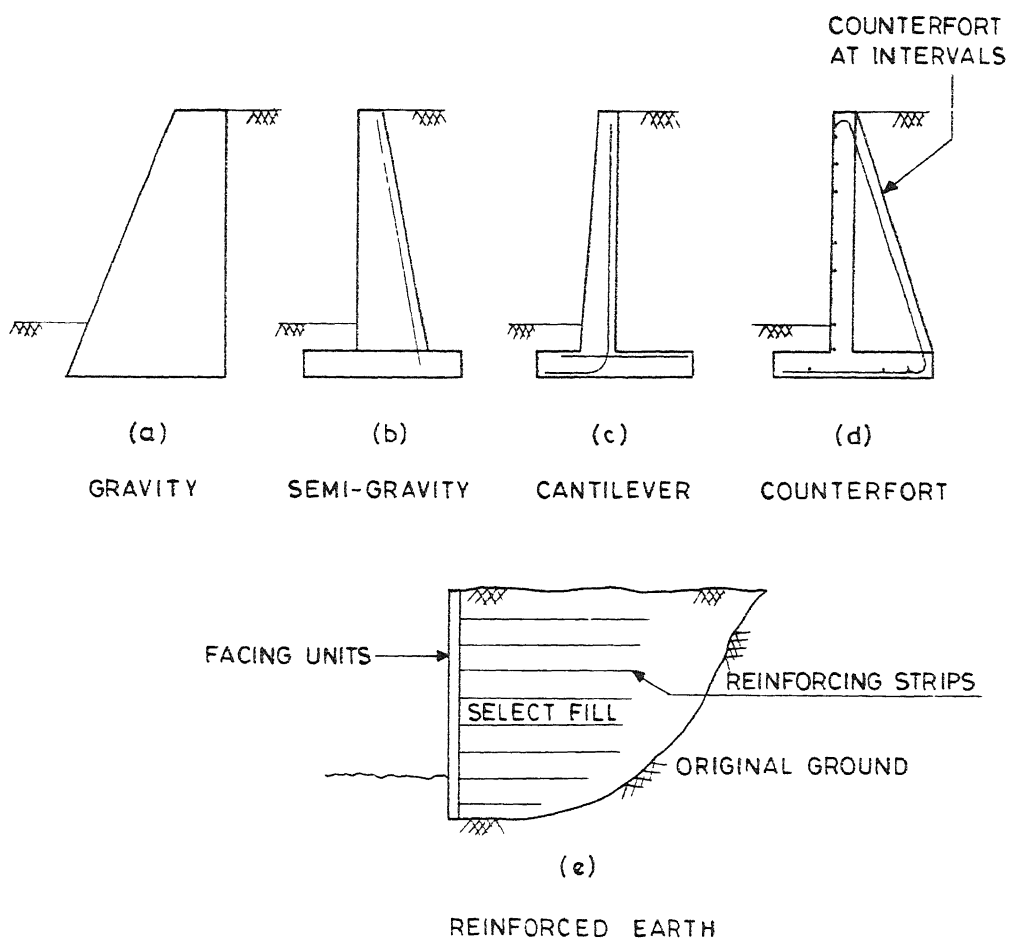


FIG.1 2 TYPES OF RETAINING WALLS

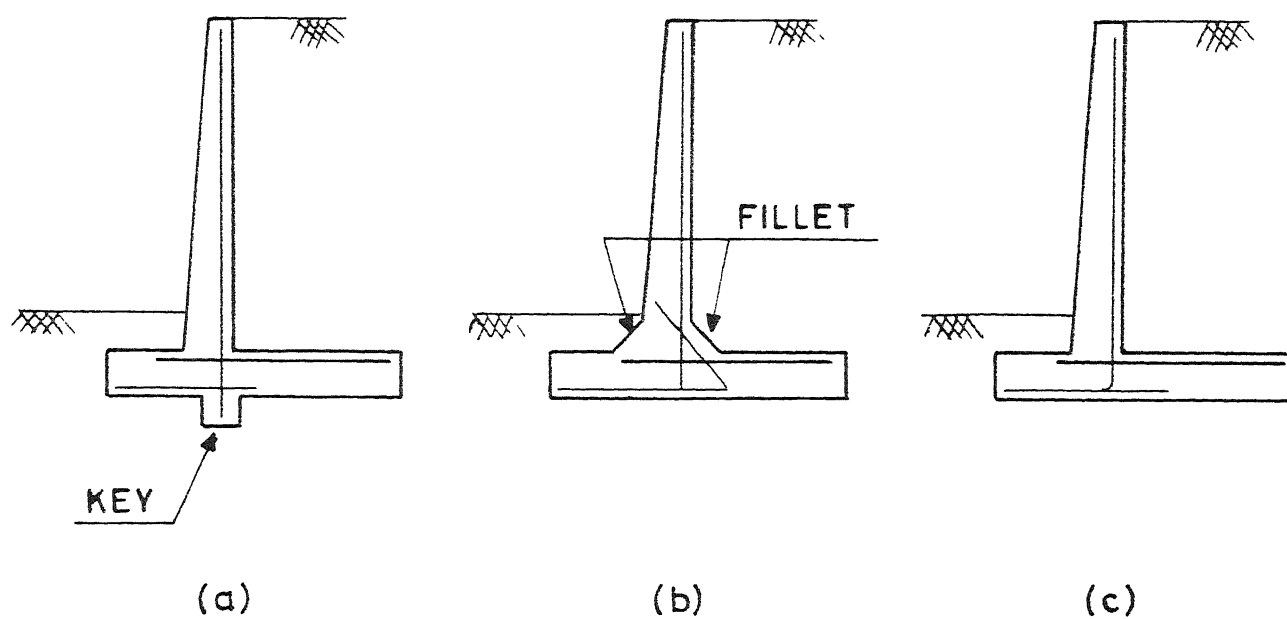
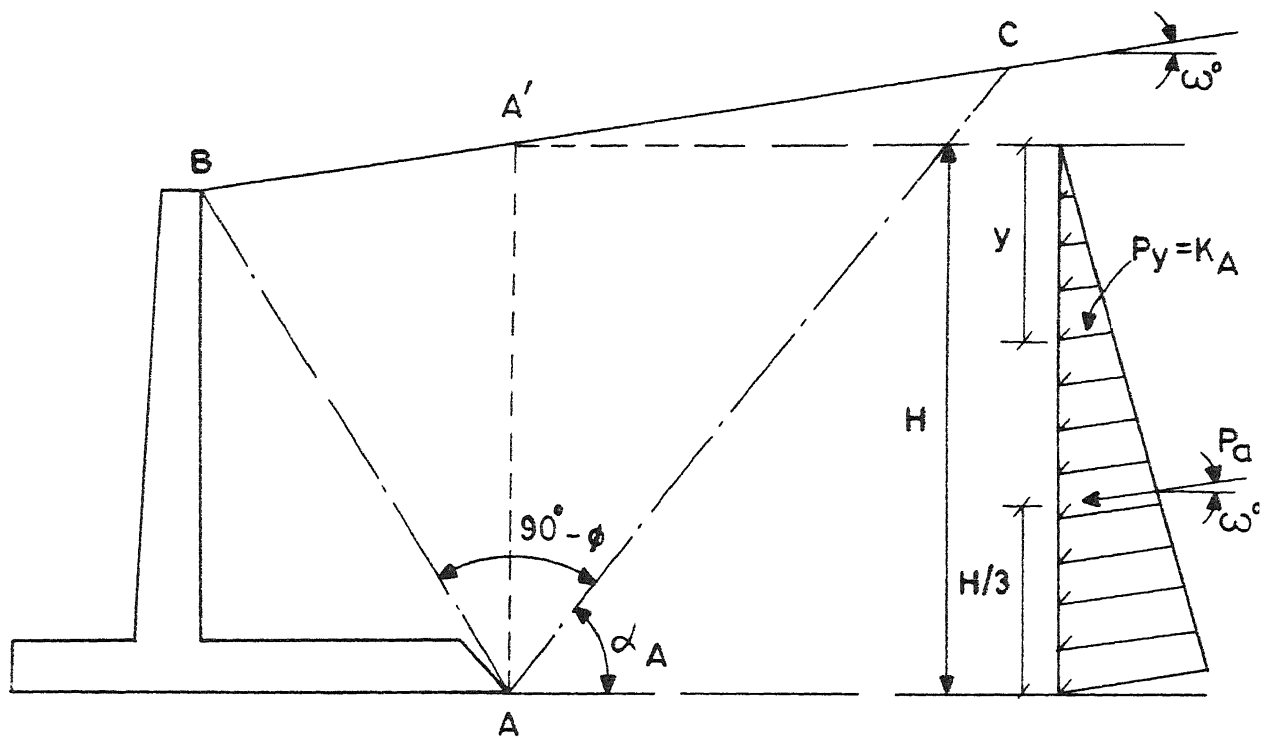


FIG.1.3: TYPES OF CANTILEVER WALL



INNER FAILURE PLANE AC
OUTER FAILURE PLANE AB

PRESSURE ON
VIRTUAL BACK AA'

FIG.1.4 : RANKINE EARTH PRESSURE THEORY

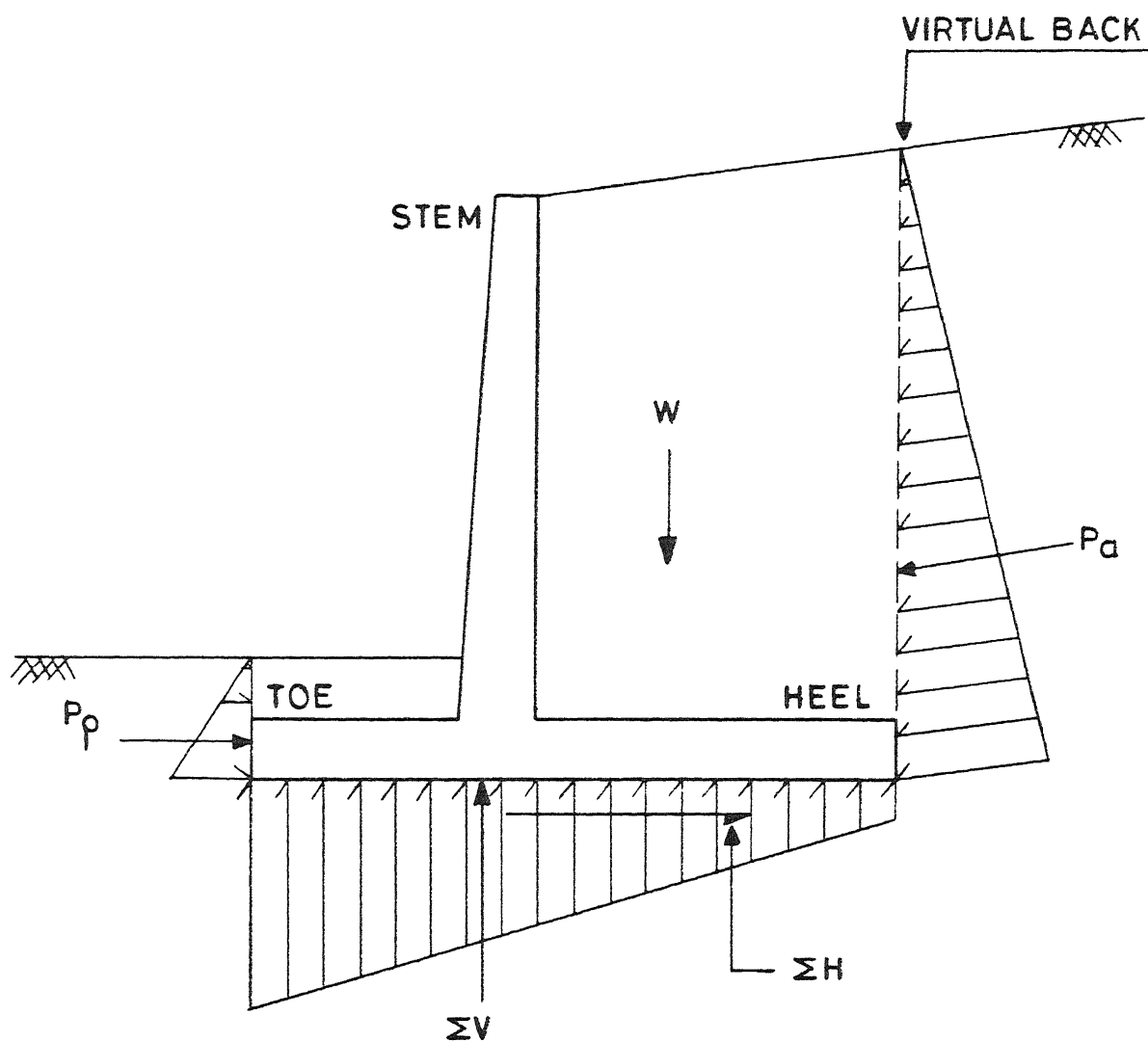


FIG . 1.5 : FORCES ACTING ON A RETAINING WALL .

CHAPTER II

METHOD OF ANALYSIS

2.1 General

The analysis of a free standing cantilever retaining wall consists of analysis of the wall stem and that of the wall footing. The following assumptions are made in the analysis:

- (i) The wall has a vertical back; The face of the wall is provided with a minimum batter of 1 in 50.
- (ii) The backfill is homogeneous, isotropic, dry, level and is of cohesionless soil
- (iii) There is no surcharge on the backfill.
- (iv) Adequate wall movement takes place to produce active state in the backfill.

2.2 Analysis of the Wall Stem

The forces acting on the wall stem are illustrated in Fig. 2.1 . They include:

- (i) The earth pressure on the stem, denoted by P_b .
- (ii) The self weight of the stem, denoted by W_{st} .

The base of the stem experiences maximum shear and maximum moment. The shear is equal to P_b . The moment, denoted by M_b , will be given by $P_b H_{st} / 3$. The direct compression and moment caused by the self weight of the stem are small quantities and are usually neglected.

2.3 Analysis of the Wall Footing

The wall footing has been analyzed by two methods They are:

- (i) The rigid foundation approach.
- (ii) The flexible foundation approach.

These methods are discussed in sections 2.3.1 and 2.3.2 respectively.

2.3.1 Rigid Foundation Approach

This approach is based on the following assumptions:

- (i) The foundation is rigid relative to the supporting soil and the compressible soil layer is relatively shallow.
- (ii) The contact pressure variation is assumed as linear, such that the centroid of the contact pressure coincides with the line of action of the resultant force of all loads acting on the foundation.

The soil pressure can be computed from principles of mechanics of materials for combined bending and axial stresses. The foundation bearing pressure at the free end of the heel and toe projections is given by

$$\begin{aligned}
 P_{\text{heel}} &= \frac{\Sigma V}{B} \left[1.0 - \frac{6e}{B} \right] \\
 P_{\text{toe}} &= \frac{\Sigma V}{B} \left[1.0 + \frac{6e}{B} \right]
 \end{aligned}
 \tag{2.1}$$

where ΣV is the vertical component of the resultant loading on the base,

B is the width of the base,

e is the eccentricity of the resultant loading.

The above expressions are valid only when the resultant loading lies within the middle third of the base. The design loadings on the heel and toe projections are shown in Fig. 2.2 . The maximum shear and maximum moment for the heel and the toe projections occur where they meet the wall stem.

The rigid foundation approach is adopted in the conventional method of analysis of the wall footing as mentioned in section 1.2 .

2.3.2 Flexible Foundation Approach

In this approach, the effects of flexural rigidity of the footing and the elasticity of the soil are considered. A number of elastic foundation models are available. In the present work, a one parameter elastic foundation model has been used. The wall footing has been analyzed as a beam on an elastic foundation. This analysis is based on the following assumptions:

- (i) A Winkler foundation model is used. It is assumed that the foundation applies only a reaction $q(x)$ normal to the beam and that $q(x)$ is directly proportional to the deflection of the beam, that is

$$q(x) = K_s y(x) \quad (2.2)$$

where $y(x)$ is the deflection,

- (ii) The foundation cannot take any tension.
- (iii) The frictional forces on the surface of contact of the beam and the foundation are not being considered.
- (iv) Shear deformation of the beam is not being considered.

The flexible foundation approach is used with the variational finite element method to analyze the wall footing. The finite

element method of analysis used in the present work is discussed in the next section

2.4 Finite Element Analysis of a Beam on a Winkler Foundation

Referring to Fig 2.3, the differential equation of a beam on a Winkler foundation is given by

$$\frac{\partial^2}{\partial x^2} \left[EI \frac{\partial^2 y}{\partial x^2} \right] + K_s y - p = 0 \quad (2.3)$$

where EI is the flexural rigidity of the beam,

p is the loading intensity on the beam.

This differential equation is to be cast in its variational form let y be the solution of (2.3) and let δy be its variation. Then, multiplying (2.3) by δy and integrating over the entire domain, we get

$$\int_0^L \left[\frac{\partial^2}{\partial x^2} \left[EI \frac{\partial^2 y}{\partial x^2} \right] + K_s y - p \right] \delta y \, dx = 0 \quad (2.4)$$

integrating (2.4) by parts, we get

$$\begin{aligned} & \left[\delta y \frac{\partial}{\partial x} \left[EI \frac{\partial^2 y}{\partial x^2} \right] \right]_0^L - \left[\delta \left(\frac{\partial y}{\partial x} \right) EI \frac{\partial^2 y}{\partial x^2} \right]_0^L + \delta \int_0^L \frac{EI}{2} \left(\frac{\partial^2 y}{\partial x^2} \right)^2 dx \\ & + \delta \int_0^L K_s \frac{y^2}{2} dx - \delta \int_0^L p y \, dx = 0 \end{aligned} \quad (2.5)$$

$$\text{let } \left. \frac{\partial}{\partial x} \left[EI \frac{\partial^2 y}{\partial x^2} \right] \right|_{x=0} = V_0^*,$$

$$\begin{aligned}
\left. \frac{\partial}{\partial x} \left[EI \frac{\partial^2 y}{\partial x^2} \right] \right|_{x=L} &= V_L^*, \\
\left[EI \frac{\partial^2 y}{\partial x^2} \right] \Big|_{x=0} &= M_0^*, \\
\left[EI \frac{\partial^2 y}{\partial x^2} \right] \Big|_{x=L} &= M_L^*, \quad (2.6)
\end{aligned}$$

Substituting (2.6) into (2.5) and simplifying, we get

$$\delta I(y) = 0 \quad \text{where}$$

$$\begin{aligned}
I(y) &= \int_0^L \left[\frac{EI}{2} \left(\frac{\partial^2 y}{\partial x^2} \right)^2 + K_s \frac{y'}{2} - p y \right] dx + V_L^* y \Big|_{x=L} \\
&\quad - M_L^* \frac{\partial y}{\partial x} \Big|_{x=L} - V_0^* y \Big|_{x=0} + M_0^* \frac{\partial y}{\partial x} \Big|_{x=0} \quad (2.7)
\end{aligned}$$

$I(y)$ is the variational functional. The highest order derivative appearing in the functional is of order two. Therefore, for completeness and compatibility, the approximating function is of the form

$$y = a_1 + a_2 x + a_3 x^2 + a_4 x^3 \quad (2.8)$$

A typical beam element is shown in Fig 2.4. The degrees of freedom at each node are the deflection, y and the slope, $\frac{\partial y}{\partial x}$. Now, eliminating the four constants a_1, a_2, a_3 , and a_4 by using the values of deflection y and slope $\frac{\partial y}{\partial x}$ at the two nodes, we get

$$y = \left\{ N^e \right\}^T \left\{ \delta^e \right\} \quad (2.9)$$

where
$$\{ N^e \}^T = \{ N_1^e, N_2^e, N_3^e, N_4^e \}$$

is the shape function vector and

$$\{ \delta^e \}^T = \left\{ y_1^e, \frac{\partial y_1^e}{\partial x}, y_2^e, \frac{\partial y_2^e}{\partial x} \right\}$$

is the element displacement vector.

Let
$$\frac{\partial^2 y}{\partial x^2} = \{ B^e \}^T \{ \delta^e \} \quad (2.10)$$

where
$$\{ B^e \} = \frac{\partial^2}{\partial x^2} \{ N^e \}$$

Let $\{ \Delta \}$ be the global displacement vector. The relation between the element displacement vector and the global displacement vector may be expressed as

$$\{ \delta^e \} = [A^e] \{ \Delta \} \quad (2.11)$$

The functional $I(y)$ has to be expressed in terms of the global displacements. Substituting (2.9) and (2.10) into (2.7) and rearranging, we get

$$\begin{aligned} I(y) = & \sum_{e=1}^{NE} \frac{1}{2} \{ \delta^e \}^T \int_{x_1^e}^{x_2^e} \left[EI \{ B^e \} \{ B^e \}^T + K_s \{ N^e \} \{ N^e \}^T \right] dx \{ \delta^e \} \\ & - \sum_{e=1}^{NE} \left[\int_{x_1^e}^{x_2^e} p \{ N^e \}^T \right] \{ \delta^e \} + V_L^* y \Big|_{x=L} - M_L^* \frac{\partial y}{\partial x} \Big|_{x=L} \\ & - V_0^* y \Big|_{x=0} + M_0^* \frac{\partial y}{\partial x} \Big|_{x=0} \end{aligned} \quad (2.12)$$

where NE denotes the number of elements

Let the term

$$V_1^* y \Big|_{x=L} - M_1^* \frac{\partial y}{\partial x} \Big|_{x=L} - V_0^* y \Big|_{x=0} + M_0^* \frac{\partial y}{\partial x} \Big|_{x=0}$$

be expressed as $\{P^*\}^T \{\Delta\}$

where $\{P^*\}$ is an external force vector.

Referring to (2.12), we define

$$[K^e] = \int_{x_1^e}^{x_2^e} \left[EI \{B^e\} \{B^e\}^T + K_s \{N^e\} \{N^e\}^T \right] dx \quad (2.13)$$

as the element stiffness matrix.

$$\{f^e\} = \int_{x_1^e}^{x_2^e} p \{N^e\} dx \quad (2.14)$$

as the element force vector.

Substituting (2.11), (2.13), (2.14) into (2.12) and further simplifying, we get

$$I(y) = \frac{1}{2} \{\Delta\}^T \left[\sum_{e=1}^{NE} [A^e]^T [K^e] [A^e] \right] \{\Delta\} - \left[\sum_{e=1}^{NE} [A^e]^T \{f^e\} + \{P^*\} \right]^T \{\Delta\} \quad (2.15)$$

$$\text{Define } [K] = \sum_{e=1}^{NE} [A^e]^T [K^e] [A^e] \quad (2.16)$$

as the global stiffness matrix,

$$\{F\} = \sum_{e=1}^{NE} [A^e]^T \{f^e\} + \{P^*\} \quad (2.17)$$

as the global force vector.

Substituting (2.16) and (2.17) into (2.15) and simplifying,

we get

$$I(y) = \frac{1}{2} \left\{ \Delta \right\}^T \left[K \right] \left\{ \Delta \right\} - \left\{ F \right\}^T \left\{ \Delta \right\} \quad (2.18)$$

$I(y)$ has thus been reduced to an ordinary function of the unknown vector $\left\{ \Delta \right\}$. Extremising $I(y)$ with respect to $\left\{ \Delta \right\}$, we get

$$\frac{\partial I(y)}{\partial \left\{ \Delta \right\}} = \frac{1}{2} \left[\left[K \right] \left\{ \Delta \right\} + \left[K \right]^T \left\{ \Delta \right\} \right] - \left\{ F \right\} = 0$$

$$\text{as } \left[K \right] \text{ is symmetric } \left[K \right] = \left[K \right]^T$$

Therefore, we get

$$\left[K \right] \left\{ \Delta \right\} = \left\{ F \right\} \quad (2.19)$$

These are the finite element equations. The element stiffness matrix and the element force vector are numerically integrated by using the Gauss - Legendre quadrature with four gauss points. The shape functions in the natural coordinates are,

$$\begin{aligned} N_1^e &= \frac{1}{4} \left[2 - 3\xi + \xi^3 \right] \\ N_2^e &= \frac{Le}{8} \left[1 - \xi - \xi^2 + \xi^3 \right] \\ N_3^e &= \frac{1}{4} \left[2 + 3\xi - \xi^3 \right] \\ N_4^e &= \frac{Le}{8} \left[1 + \xi - \xi^2 - \xi^3 \right] \end{aligned} \quad (2.20)$$

where Le denotes the element length

Once the global displacement vector $\left\{ \Delta \right\}$ has been found, the

member end actions are found by using the relation

$$\left[K^e \right] \left\{ \delta^e \right\} - \left\{ f^e \right\} = \left\{ f \right\} \quad (2.21)$$

where

$$\left\{ f \right\} = \left\{ V_1^e, M_1^e, V_2^e, M_2^e \right\}$$

V_i^e = shear at the i^{th} node of member,

M_i^e = moment at the i^{th} node of member

The maximum shear and maximum moment for the elements of the heel and the toe projections is found out. The maximum deflection of the footing, denoted by y_{max} , is found out. This on being multiplied by the subgrade modulus, k_s , yields the maximum foundation pressure, P_{max} . These quantities are considered for the optimum design of the retaining wall. In the event of tension being developed in the foundation, an iterative scheme is adopted. At first, the nodes where tension develops, are identified. The Winkler modulus, K_s , is set to zero at these nodes. The system is reanalyzed. Convergence takes place when no further nodes develop tension.

2.5 Discretization

Fig. 2.5 illustrates the discretization adopted for the footing. It also shows the loads acting on the footing of the retaining wall. The mesh consists of twenty finite elements. Six and twelve elements are used for the toe and heel projections respectively. Two elements are used for the joint where the stem, toe projection and heel projection meet. The dead load of the stem, W_{st} , and the moment due to lateral earth pressure, M_b , are applied at node no. 8 in the mesh. The location of node 8 is where

the line of action of W_{st} meets the foundation. Since the joint is rigid, the flexural rigidity of the two elements that comprise it is taken to be a thousand times that of the elements in the heel projection.

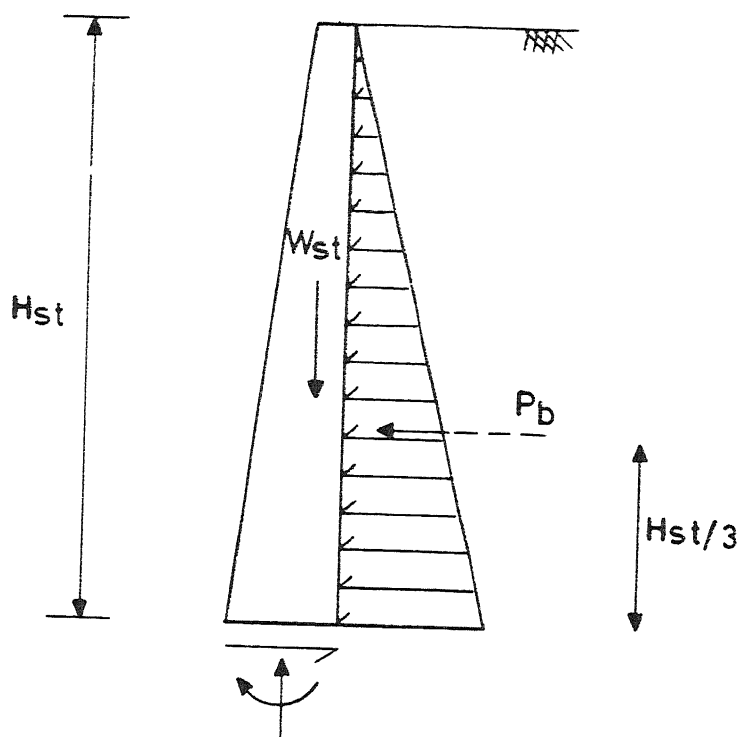


FIG. 2.1: FORCES ACTING ON THE WALL STEM .

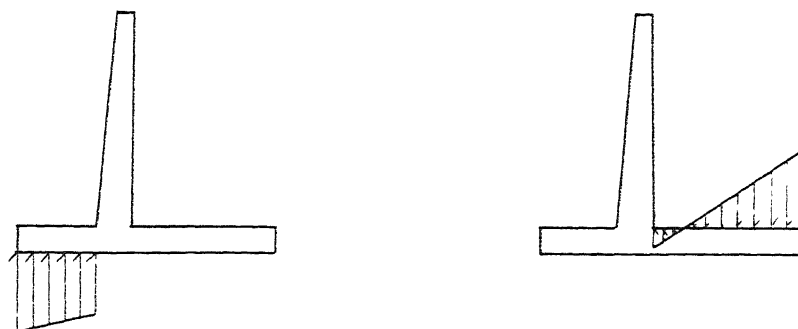


FIG.2 2 DESIGN LOADING ON THE TOE AND HEEL PROJECTIONS

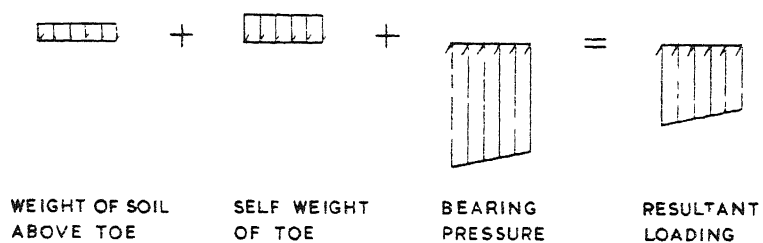


FIG 2 2 (a) RESULTANT LOADING ON THE TOE PROJECTION

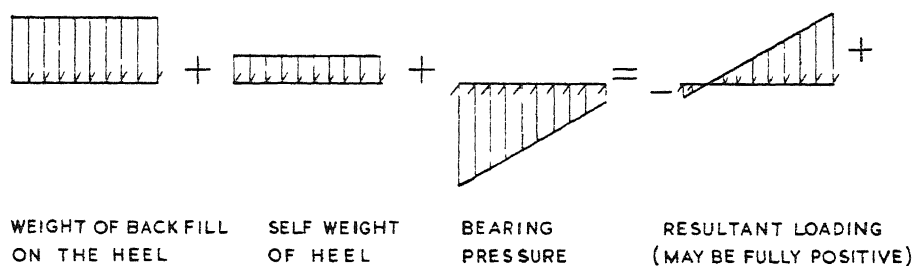
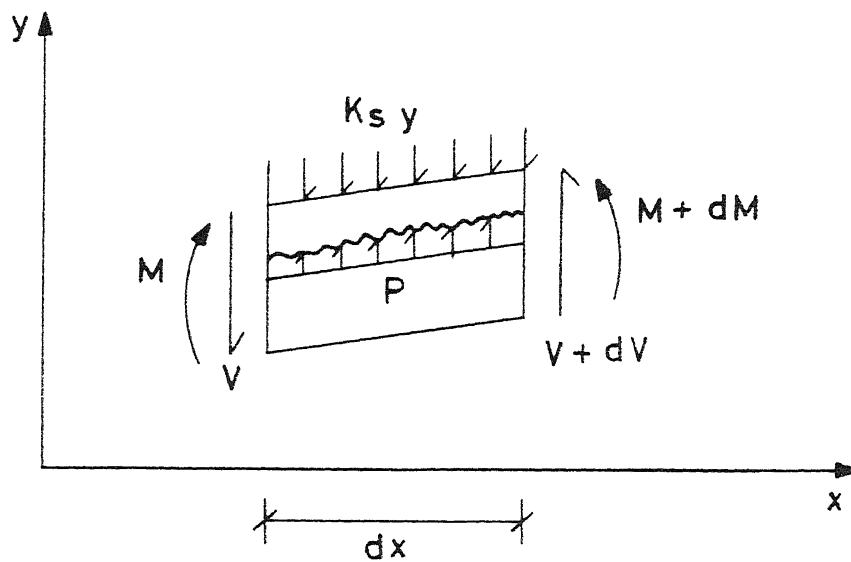


FIG 2 2 (b) RESULTANT LOADING ON THE HEEL PROJECTION



$$\frac{dV}{dx} = (K_s y - P)$$

$$\frac{dM}{dx} = -V$$

$$EI \frac{d^2 y}{dx^2} = M$$

Differential Equation is $\frac{d^2}{dx^2} \left[EI \frac{d^2 y}{dx^2} \right] + K_s y - P = 0$

FIG. 2.3: DIFFERENTIAL EQUATION FOR A BEAM ON A WINKLER FOUNDATION.

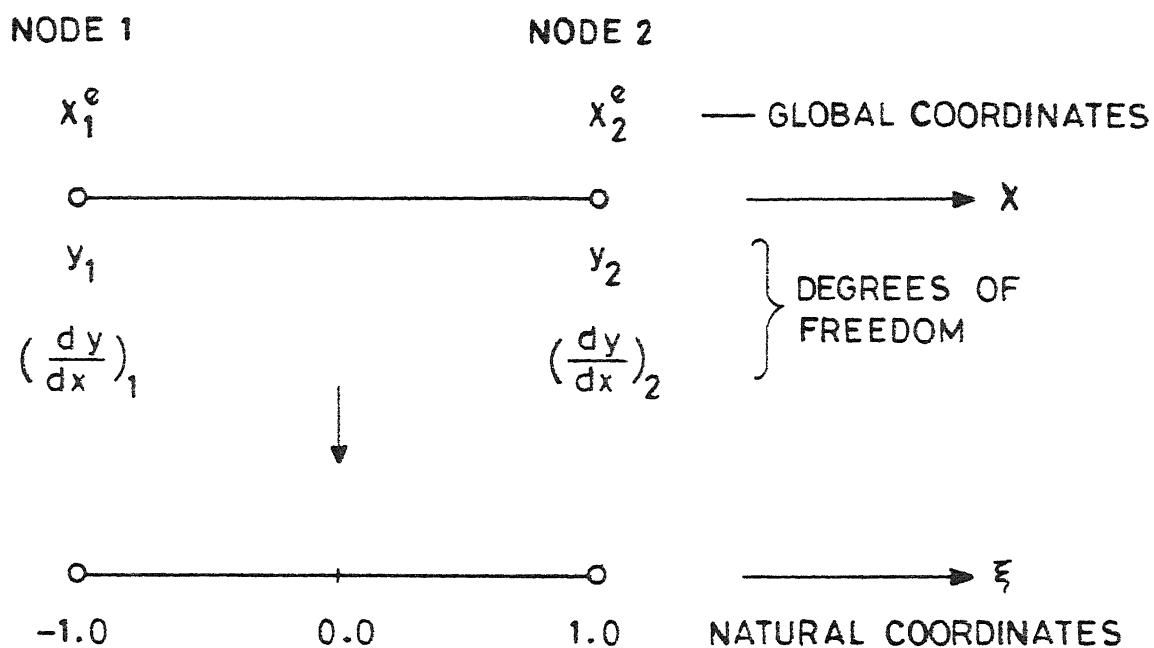


FIG. 2.4: A TYPICAL BEAM ELEMENT

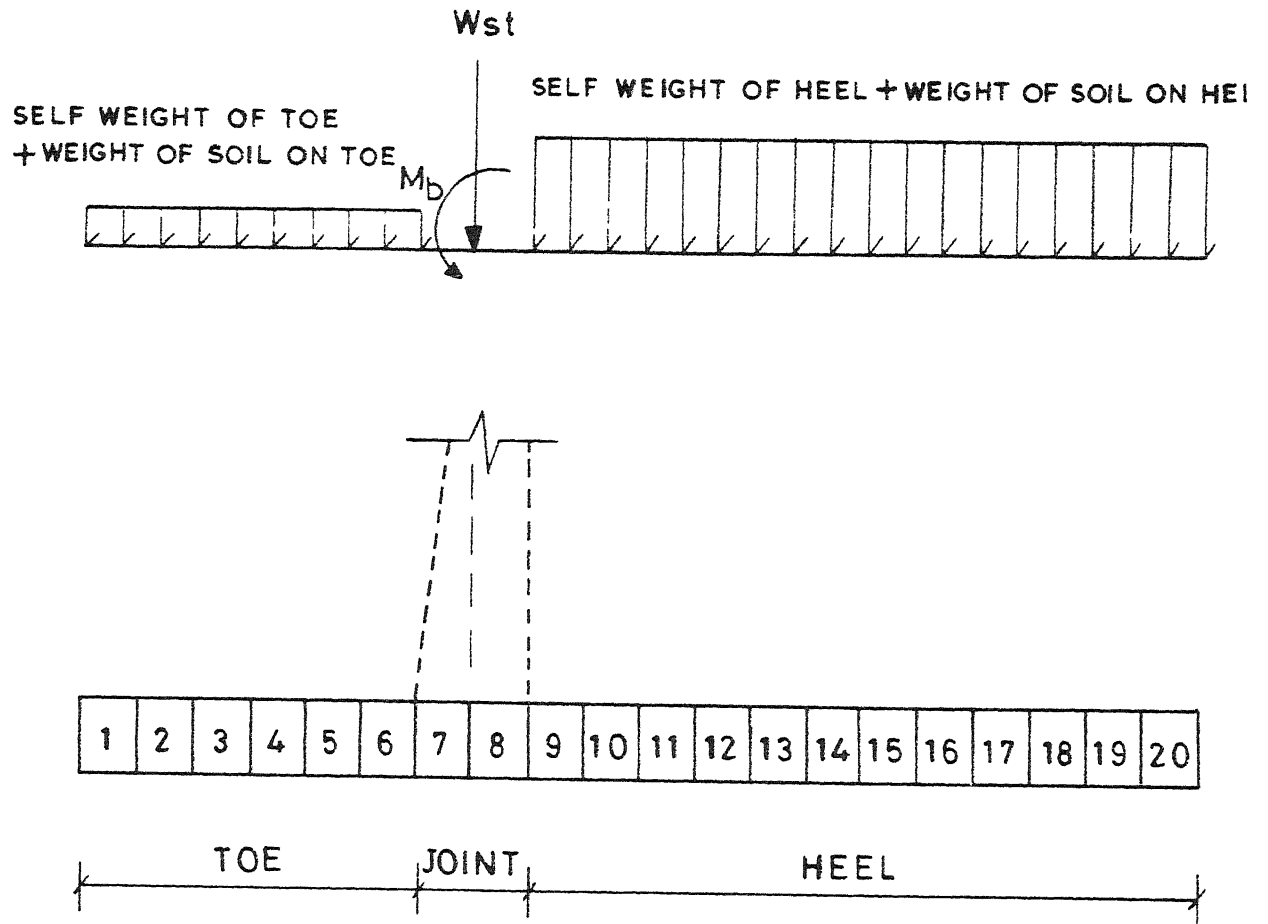


FIG . 2 . 5 : **DISCRETIZATION AND LOADING ON FOOTING**

CHAPTER III

FORMULATION OF THE OPTIMUM DESIGN PROBLEM

3.1 Introduction

The present work addresses itself to the optimum design of a free standing cantilever retaining wall on (i) rigid and (ii) flexible, foundations. The formulation of the optimum design problem leads to the following nonlinear programming problem ,

find the design vector $X = \{ X_1, X_2, X_3, \dots, X_N \}^T$

to minimize $F(X)$

subject to $g_j(X) \leq 0$, $j = 1, 2, \dots, m$,

where N is the number of design variables,

m is the total number of inequality constraints,

$F(X)$ is the objective function,

$g_j(X)$ is the j^{th} inequality constraint

3.2 Design Variables and Preassigned Parameters

Referring to Fig. 3.1, the design variables in the problem are as follows :

- X_1 — overall depth at the base of the stem,
- X_2 — overall depth of the toe projection,
- X_3 — length of the toe projection,
- X_4 — length of the heel projection,
- X_5 — overall depth of the heel projection,
- X_6 — percentage of main steel in the heel projection,
- X_7 — percentage of main steel at the base of the stem,
- X_8 — percentage of main steel in the toe projection.

The preassigned parameters are the top width of the wall, denoted by T , the overall height of the wall, denoted by H_w , and the properties of concrete, steel and soil

3.3 Constraints

The design of a retaining wall must satisfy the following requirements :

- (a) The soil containing the wall must be stable,
- (b) The retaining wall must be stable,
- (c) The wall must have adequate structural strength

In the present work, the working stress method of I.S. 456 - 1978, has been used to determine the structural strength of the wall

The requirements, (a), (b), and (c), listed above, give rise to the following behavior constraints

(1) Safety against overturning about the toe

Let W denote the weight of the wall and that of the soil above the heel and toe projections. Let X_w denote the distance between the line of action of W and the toe. The resisting moment is then equal to $W X_w$. The overturning moment is given by

$$P_h \bar{h} - P_v B$$

where P_h and P_v are the horizontal and vertical components of the resultant active earth pressure against the virtual back of the wall, \bar{h} is the height above foundation level at which P_h cuts the virtual back. The factor of safety against overturning is then given by the ratio ,

$$\left[\frac{W X_w}{P_h \bar{h} - P_v B} \right]$$

The factor of safety must be at least 2.0. The constraint is

$$g_1(X) = 1.0 - \frac{1}{2} \left[\frac{W X_w}{P_h \bar{h} - P_v B} \right] \quad (3.1)$$

(ii) Safety against Sliding

The external force causing sliding of the wall is P_h . The force that resists the sliding is given by

$$\left[\Sigma V \tan \phi_b + c_b B + 2/3 P_p \right]$$

It is assumed that only two thirds of the passive force P_p is effective in resisting sliding. The factor of safety must be at least 1.5. The constraint is

$$g_2(X) = 1.0 - \frac{1}{1.5} \left[\frac{\Sigma V \tan \phi_b + c_b B + 2/3 P_p}{P_h} \right] \quad (3.2)$$

(iii) Limit on the eccentricity of the resultant loading on the foundation

The eccentricity, denoted by e , must be limited to one sixth of the base width to prevent any tension from developing in the foundation. The constraint is

$$g_3(X) = \left[\frac{e}{B/6} \right] - 1.0 \quad (3.3)$$

(iv) Maximum pressure on the foundation

Let P_{\max} denote the maximum foundation bearing pressure. This

must be less than A_{bc} , the allowable bearing capacity of the soil, which is found by using the Meyerhof equations as explained in Appendix A. The constraint is

$$g_4(X) = \left[\frac{P_{\max}}{A_{bc}} \right] - 1.0 \quad (3.4)$$

(v) Safety against slip circle failure

Referring to Fig. 3.2, the factor of safety against slip circle failure along a trial arc is given by

$$\left[\frac{\sum \sigma_n \tan \phi + c l}{\sum T} \right]$$

where $\sum T = \frac{W' r'}{R} \quad (3.5)$

The method used to compute the factor of safety is explained in Appendix B. The factor of safety must be at least 2.0. The constraint is

$$g_5(X) = 1.0 - \frac{1}{2.0} \left[\frac{\sum \sigma_n \tan \phi + c l}{\sum T} \right] \quad (3.6)$$

(vi) Moment of resistance of stem at the base

The bending moment at the stem base is given by

$$M_b = \frac{P_b H_{st}}{3.0} \quad (3.7)$$

The resisting moment is given by

$$R_m = \frac{X_7 \sigma_{st} d_s^2 \left[1.0 - \eta/3.0 \right]}{100.0} \quad (3.8)$$

where,

$$\eta = \frac{X_7 m_d}{100.0} \left[-1.0 + \left[1.0 + \frac{200.0}{m_d X_7} \right]^{1/2} \right] \quad (3.9)$$

m_d is the modular ratio,

σ_{st} is the permissible tensile stress in the steel,

d_s is the effective depth at the stem base.

The resisting moment must be greater than the bending moment. The constraint is

$$g_6(X) = 1.0 - \left[\frac{R_m}{M_b} \right] \quad (3.10)$$

(vii) Shear resistance of the stem at the base

The shear force at the base of the stem is P_b . The shear resistance per meter length at the base of the stem is $\tau_c d_s$. The shear resistance must be greater than the shear force. The constraint is

$$g_7(X) = \left[\frac{\tau_c d_s}{P_b} \right] - 1.0 \quad (3.11)$$

(viii) Moment of resistance of the heel projection

Let the maximum bending moment on the heel projection be M_h . The resisting moment is given by

$$R_m = \frac{X_6 \sigma_{st} d_h^2 \left[1.0 - \eta/3.0 \right]}{100.0} \quad (3.12)$$

where,

$$\eta = \frac{X_6 m_d}{100.0} \left[-1.0 + \left[1.0 + \frac{200.0}{m_d X_6} \right]^{1/2} \right] \quad (3.13)$$

d_h is the effective depth of the heel projection.

The moment of resistance must be greater than the bending moment. The constraint is

$$g_8(X) = \left[\frac{R_m}{M_h} \right] - 1.0 \quad (3.14)$$

(ix) Shear resistance of the heel projection

Let the shear force at the junction of the heel projection and the stem be V_h . The shear resistance per meter length of the heel projection at this section is $\tau_c d_h$. The shear resistance must be greater than the shear force. The constraint is

$$g_9(X) = \left[\frac{\tau_c d_h}{V_h} \right] - 1.0 \quad (3.15)$$

(x) Moment of resistance of the toe projection

Let the maximum bending moment on the toe projection be M_t . The resisting moment is given by

$$R_m = \frac{X_8 \sigma_{st} d_t^2 \left[1.0 - \eta/3.0 \right]}{100.0} \quad (3.16)$$

where

$$\eta = \frac{X_8 m_d}{100.0} \left[-1.0 + \left[1.0 + \frac{200.0}{m_d X_8} \right]^{1/2} \right] \quad (3.17)$$

d_t is the effective depth of the toe projection.

The moment of resistance must be greater than the bending moment. The constraint is

$$g_{10}(X) = \left[\frac{R_m}{M_t} \right] - 1.0 \quad (3.18)$$

(xi) Shear resistance of the toe projection

Let the shear force at the junction of the toe projection and the stem be V_t . The shear resistance per meter length of the toe projection at this section is $\tau_c d_t$. The shear resistance must be greater than the shear force. The constraint is

$$g_{11}(X) = \left[\frac{\tau_c d_t}{V_t} \right] - 1.0 \quad (3.19)$$

All the above eleven behavior constraints are considered when rigid foundation behavior is assumed. The constraint for limit on the eccentricity of the resultant loading on the foundation, $g_3(X)$, prevents tension from being developed for rigid foundation behavior. This constraint, however, does not arise for flexible foundation behavior. The maximum shear forces, bending moments and the maximum foundation pressure are obtained from analysis carried out by the finite element method described in section 2.4 .

3.4 Side Constraints

The side constraints on the design variables are based on suggestion by Bowles (1988), Ferguson (1987), Huntington (1957) and I S. 456 - 1978. Let X_{iL} denote lower bound and X_{iU} denote upper bound on the i^{th} design variable. The following bounds have

been considered in the present work

$$\begin{array}{ll}
 X_{1L} = T + \frac{H_w}{50} & X_{1U} = \frac{H_w}{6} \\
 X_{2L} = 0.150 & X_{2U} = 0.15 H_w \\
 X_{3L} = 0.075 H_w & X_{3U} = 0.40 H_w \\
 X_{4L} = 0.10 H_w & X_{4U} = 0.60 H_w \\
 X_{5L} = 0.150 & X_{5U} = 0.15 H_w \\
 X_{6L} = Astmin & X_{6U} = Astmax \\
 X_{7L} = Astmin & X_{7U} = Astmax \\
 X_{8L} = Astmin & X_{8U} = Astmax
 \end{array}$$

(3 20)

where

H_w is the total height of the wall,

T is the top width,

$Astmin$ is the minimum percentage of main steel permissible,

$Astmax$ is the maximum percentage of main steel permissible.

3.5 Objective function

The objective function is the material cost of the retaining wall per meter length, which can be expressed as

$$F(X) = U_c V_c + U_s W_s \quad (3.21)$$

where U_c is the unit cost of concrete in Rs/m³,

V_c is the total volume of concrete in m³,

U_s is the unit cost of steel in Rs/ton ,

W_s is the total weight of the steel reinforcement in tons.

The percentage of main steel at the base of the stem is X_7 .

As the bending moment in the stem rapidly diminishes towards the top, 50% and 75% of the main steel X_7 is assumed to be curtailed at heights hc_1 and hc_2 above the base respectively. The theoretical points of cut off are found keeping in view the requirements of minimum main steel in the section. Thus, the volume of main steel in the stem is

$$V_{sm} = \left[0.5 hc_1 + 0.25 (hc_2 + Hst) \right] \frac{X_7 d_s}{100.0} \quad (3.22)$$

For temperature and shrinkage, the horizontal reinforcement required is 0.25% of the gross cross sectional area of the stem. In addition, vertical reinforcement equal to the minimum percentage of steel permissible in a section, that is, A_{stmin} , is to be provided. Thus, the distribution steel in the stem is

$$V_{sd} = \frac{(T + X_1)}{2.0} Hst \frac{(0.25 + A_{stmin})}{100.0} \quad (3.23)$$

The volume of main steel in the heel projection is

$$V_{hm} = \frac{X_4 X_6 d_h}{100.0} \quad (3.24)$$

The distribution steel in the heel projection is

$$V_{hd} = X_4 X_5 \frac{A_{stmin}}{100.0} \quad (3.25)$$

The volume of main steel in the toe projection is

$$V_{tm} = \frac{X_3 X_8 d_t}{100.0} \quad (3.26)$$

The distribution steel in the toe projection is

$$V_{td} = X_2 X_3 \frac{A_{stmin}}{100.0} \quad (3.27)$$

Let V_{Ld} denote the additional volume of steel required for development lengths, dower bars and lap splices. Then, the total volume of steel is,

$$V_{steel} = V_{sm} + V_{sd} + V_{hm} + V_{hd} + V_{tm} + V_{td} + V_{Ld} \quad (3.28)$$

The total weight of steel, denoted by WS , is

$$WS = V_{steel} \times \gamma_{st} \quad \text{tons} \quad (3.29)$$

where γ_{st} is the unit weight of steel in tons/m^3 .

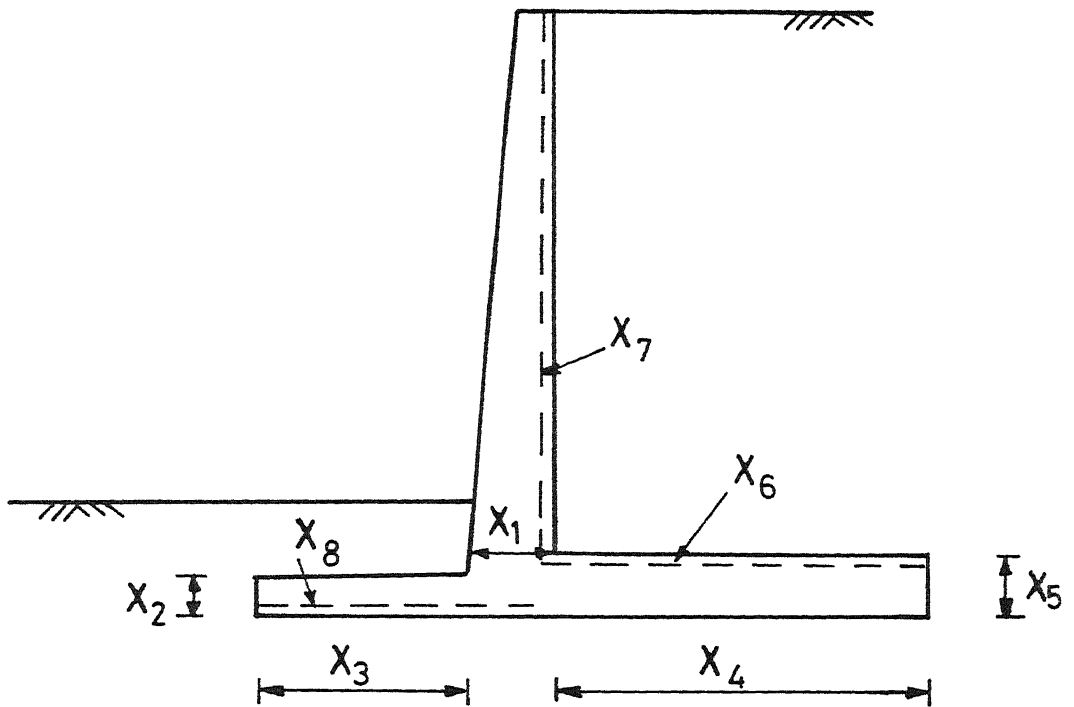
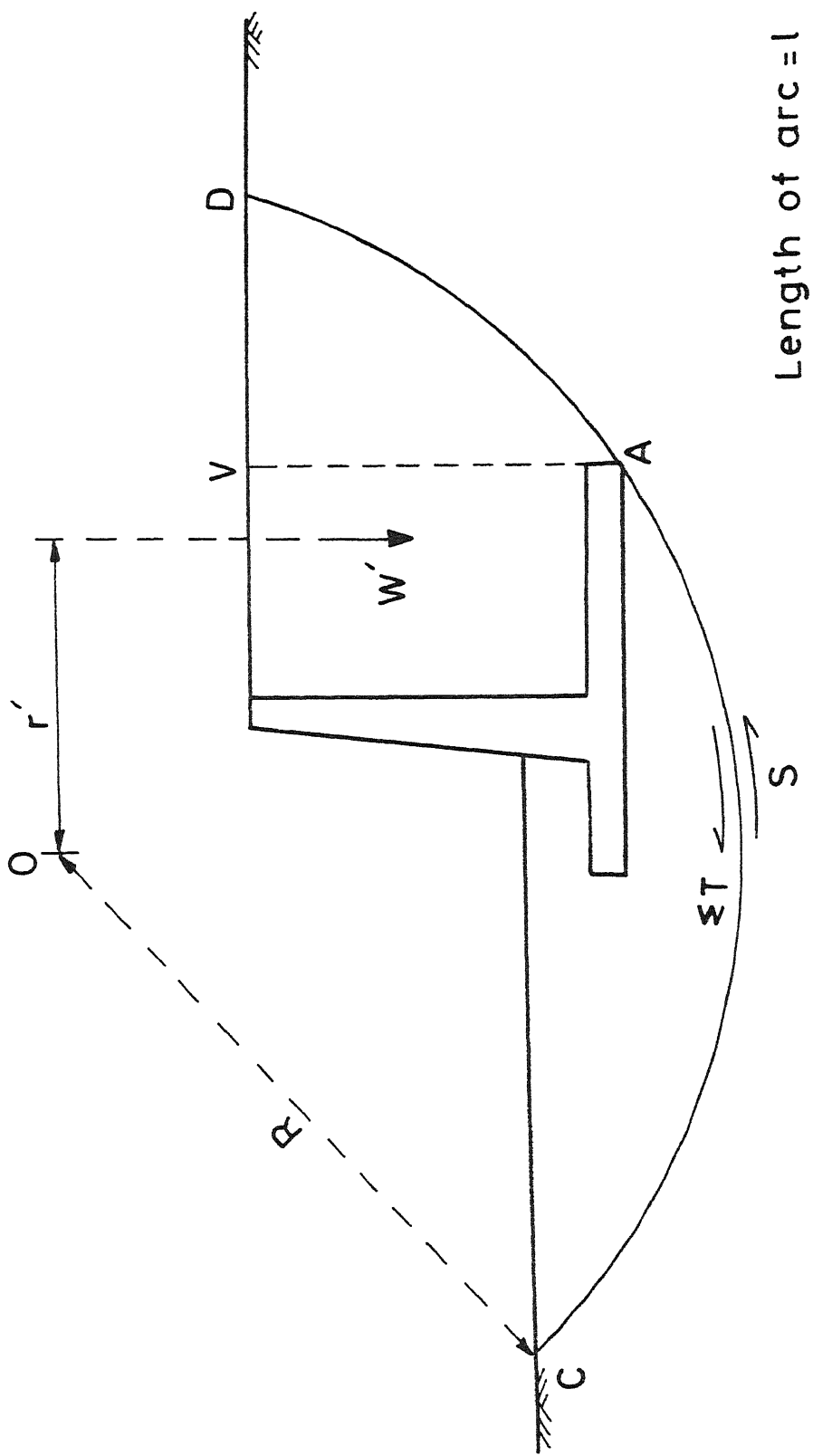


FIG. 3.1: DESIGN VARIABLES



$$S = \Sigma \sigma' \tan \phi + cl$$

$$\Sigma T = W' r' / R$$

FIG. 3.2: STABILITY AGAINST SLIP CIRCLE FAILURE

CHAPTER IV

METHOD FOR OPTIMUM DESIGN

4.1 General

There are many methods available for the solution of a constrained nonlinear optimum design problem. All these methods can be classified into two broad categories, namely, the direct methods and the indirect methods. Among the direct methods are

- (i) The sequential linear programming method,
- (ii) The gradient projection method of Rosen,
- (iii) The feasible direction method of Zoutendijk,
- (iv) The generalized reduced gradient method.

The indirect methods are basically sequential unconstrained minimization techniques like the penalty function methods and the augmented lagrange multiplier method.

The interior penalty function method has been used in this work. It is reliable and is easy to implement.

4.2 Interior Penalty Function Method

In this method, the constrained minimization problem is transformed into a sequence of unconstrained minimization problems by adding a penalty term to the original objective function. The penalty function suggested by Fiacco and McCormick is given by

$$\Phi(X, r) = F(X) - r \sum_{j=1}^m \frac{1}{g_j(X)} \quad (4.1)$$

where $\Phi(X, r)$ is the penalty function and r is the penalty

parameter.

The flowchart for this algorithm is illustrated in Fig.4.1.

The algorithm is summarized as follows:

- (i) Start with an initial feasible point $X^{(0)}$ satisfying all the constraints with strict inequality sign, that is,
 $g_j(X^{(0)}) < 0$ for $j = 1, 2, \dots, m$.
- (ii) Select the initial value of the penalty parameter r such that the contribution of the objective function and the penalty term to the penalty function $\Phi(X, r)$ becomes equal.
- (iii) Minimize $\Phi(X, r)$ by using an unconstrained optimization method and obtain X_m .
- (iv) Check for convergence of X_m to the optimum.
- (v) If the convergence criterion is not satisfied, set $r = C'r$, where $C' < 1$ and repeat from step (iii).

Convergence criteria . Two termination criteria are used. The first is to compute the relative difference

$$\delta = \frac{\left| F_{\min}(r_{i-1}) - F_{\min}(r_i) \right|}{\left| F_{\min}(r_i) \right|} \quad (4.2)$$

and stop when this value drops below a certain fraction ϵ_1 . The second is when

$$\Delta = \left[\sum_{j=1}^m \Delta_j^2 \right]^{1/2} \leq \epsilon_2 \quad (4.3)$$

where $\Delta = X_m(r_{i-1}) - X_m(r_i)$ (4.4)

Δ_j is the j^{th} component of Δ

The algorithm terminates when either criterion is satisfied in at least two successive iterations

4.3 Unconstrained Minimization

The unconstrained minimum of $\Phi(X, r)$ is obtained by the Davidon - Fletcher - Powell variable metric method. The iterative procedure of this method is illustrated in Fig 4.2. It is summarized as follows :

- (i) Start with an initial design $X^{(0)}$ and a symmetric, positive definite matrix $A^{(0)}$, which may be taken as the identity matrix. Specify a convergence parameter ϵ . Set $K = 0$. Compute the gradient vector as

$$C^{(0)} = \nabla F(X^{(0)}) \quad (4.5)$$

- (ii) Calculate the norm of the gradient vector as $\|C^{(K)}\|$. If $\|C^{(K)}\| < \epsilon$, then stop the iterative process, otherwise continue.
- (iii) Calculate the search direction as

$$S^{(K)} = -A^{(K)} C^{(K)} \quad (4.6)$$

- (iv) Compute the optimum step size $\alpha_K = \alpha^*$ so as to minimize $F(X^{(K)} + \alpha S^{(K)})$. α_K is found by linear minimization along the direction $S^{(K)}$.
- (v) Update the design as

$$X^{(K+1)} = X^{(K)} + \alpha_K S^{(K)} \quad (4.7)$$

(vi) Update the matrix $A^{(K)}$ as

$$A^{(K+1)} = A^{(K)} + M^{(K)} + N^{(K)}, \quad N \times N \text{ matrices, where}$$

$$M^{(K)} = \frac{\alpha_k S^{(K)} S^{(K)T}}{\begin{bmatrix} S^{(K)T} & Y^{(K)} \end{bmatrix}}, \quad (4.8)$$

$$N^{(K)} = \frac{Z^{(K)} Z^{(K)T}}{\begin{bmatrix} Y^{(K)} & Z^{(K)} \end{bmatrix}}, \quad (4.9)$$

with

$$Y^{(K)} = C^{(K+1)} - C^{(K)}$$

$$C^{(K+1)} = \nabla F(X^{(K+1)})$$

$$Z^{(K)} = A^{(K)} Y^{(K)} \quad (4.10)$$

(vi) Set $K = K + 1$ and repeat from step (ii).

In order to avoid any numerical difficulties the matrix $A^{(K)}$ is set to $A^{(0)}$ after every 8 iterations

4.4 Linear Minimization

Linear minimization is carried out by the three point quadratic interpolation method. The flowchart for this method is illustrated in Fig 4.3. In the first phase of this method, bounds are found on the minimum with due care taken to avoid any constraint violations. In the second phase, the objective function $F(\alpha)$ is locally approximated by a quadratic

$$H(\alpha) = a + b\alpha + c\alpha^2 \quad (4.11)$$

the minimum of which occurs where

$$\frac{dH}{d\alpha} = b + 2c\alpha = 0, \quad \text{or} \quad \alpha^* = -b/2c \quad (4.12)$$

The values of the constants, a, b, and c, are obtained by equating the value of $H(\alpha)$ with that of $F(\alpha)$ at three points, α_1 , α_2 , and α_3 , and then solving the resulting equations. Convergence takes place when

$$\delta = \frac{|H(\alpha^*) - F(\alpha^*)|}{|H(\alpha^*)|} \quad (4.13)$$

becomes less than a certain fraction ϵ . If convergence is not satisfied, the quadratic $H(\alpha)$ is refit through three of the four available points and the process repeated.

Computer implementation of the interior penalty function method is done in double precision arithmetic. The gradient calculations are done initially by the forward difference method and later by the central difference method.

4.5 Initial Feasible Design

Fig.4.4 illustrates the starting point that is in general feasible for cohesionless soils. This has been taken from Bowles (1988).

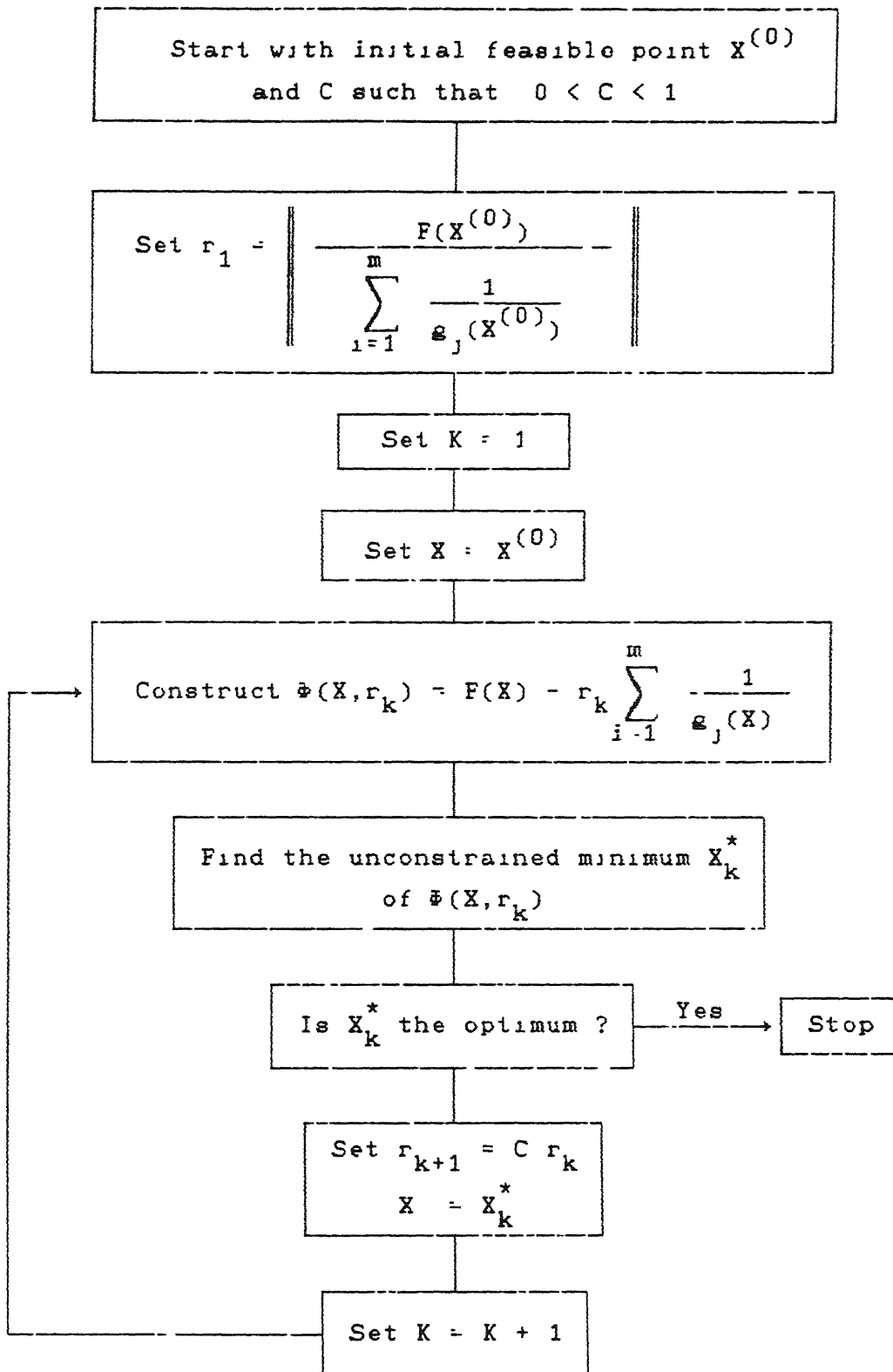


FIG. 4.1: FLOW CHART FOR INTERIOR PENALTY FUNCTION METHOD

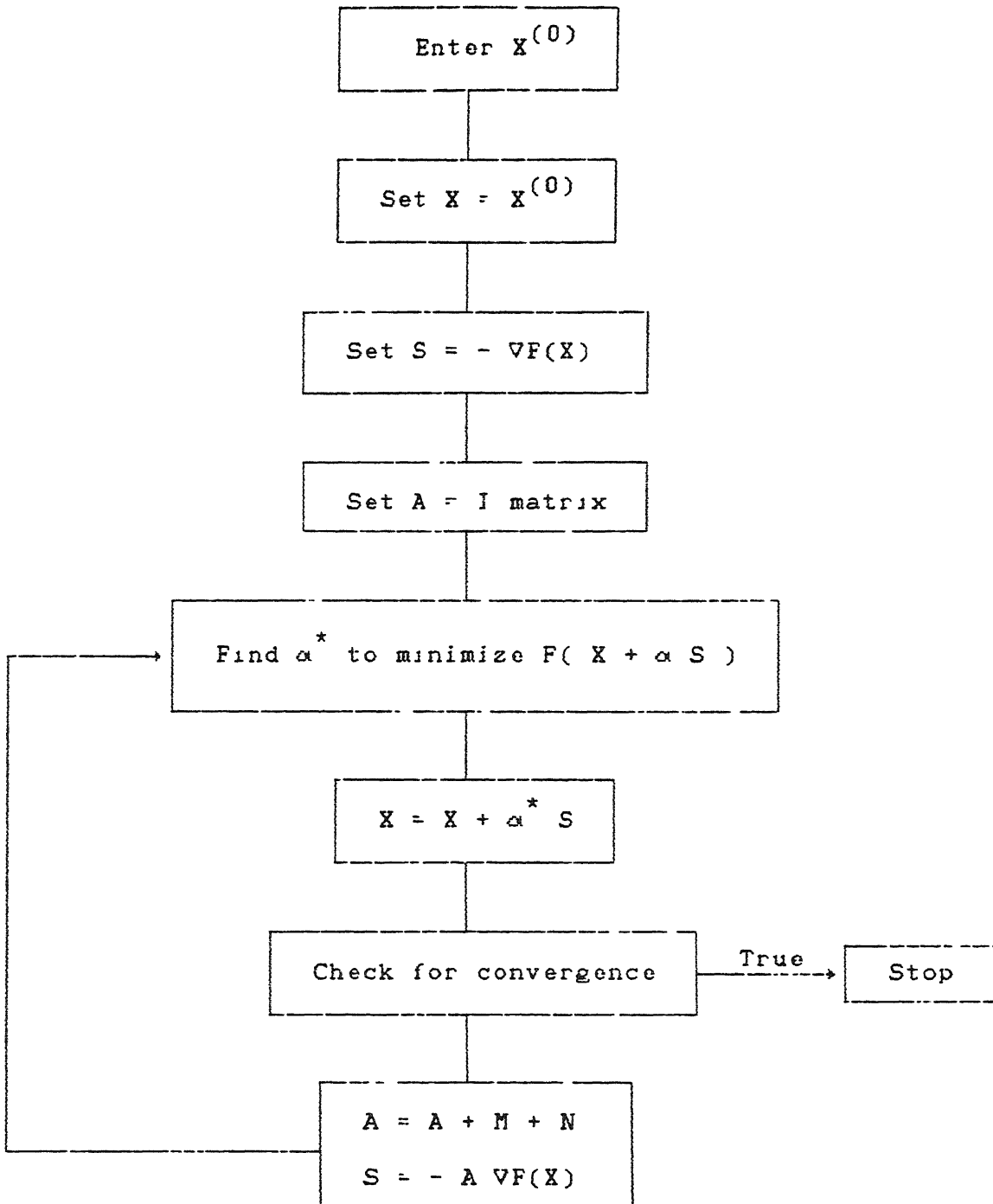


FIG. 4.2: FLOW CHART FOR DAVIDON-FLETCHER-POWELL METHOD

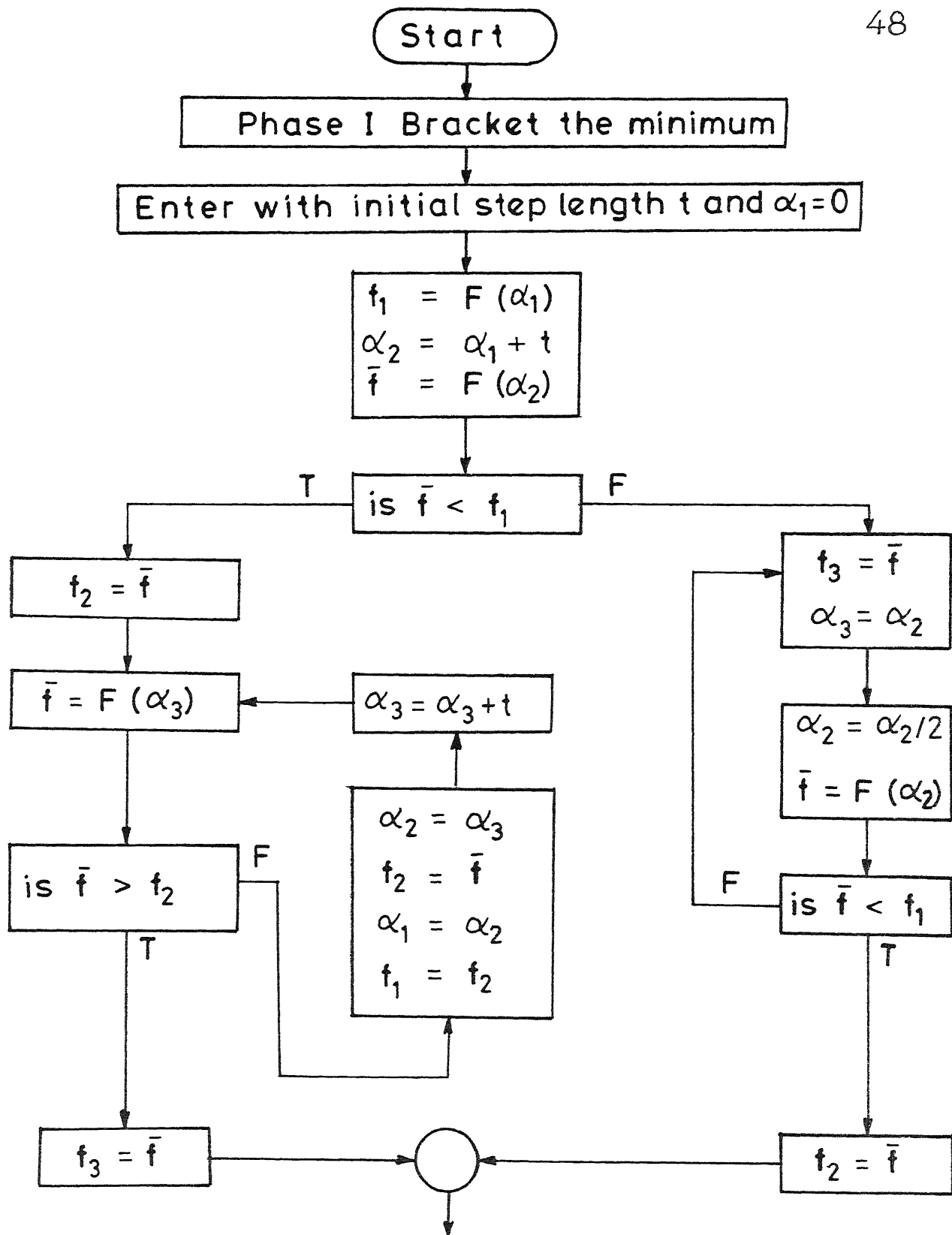


FIG 4.3: FLOW CHART FOR QUADRATIC INTERPOLATION

Phase II: Fitting the Quadratic $H(\alpha)$

$$H(\alpha) = a + b\alpha + c\alpha^2$$

find coefficients a, b and c using $\alpha_1, \alpha_2, \alpha_3$ and $f(\alpha_1), f(\alpha_2), f(\alpha_3)$

$$\alpha^* = -b/2C$$

$$\text{is } \left\| \frac{H(\alpha^*) - F(\alpha^*)}{F(\alpha^*)} \right\| < \epsilon$$

T

α^* optimum

EXIT

F

$$f^* = F(\alpha^*)$$

T

$$\text{is } \alpha_2 < \alpha^*$$

F

T

$$\text{is } f_2 < f^*$$

F

T

$$\text{is } f_2 < f^*$$

F

$$\begin{aligned} x_1 &= \alpha_1 \\ x_2 &= \alpha_2 \\ x_3 &= \alpha^* \end{aligned}$$

$$\begin{aligned} \alpha_1 &= \alpha_2 \\ \alpha_2 &= \alpha^* \\ \alpha_3 &= \alpha_3 \end{aligned}$$

$$\begin{aligned} \alpha_1 &= \alpha^* \\ \alpha_2 &= \alpha_2 \\ \alpha_3 &= \alpha_3 \end{aligned}$$

$$\begin{aligned} \alpha_1 &= \alpha_1 \\ \alpha_3 &= \alpha_2 \\ \alpha_2 &= \alpha^* \end{aligned}$$

GO TO 10

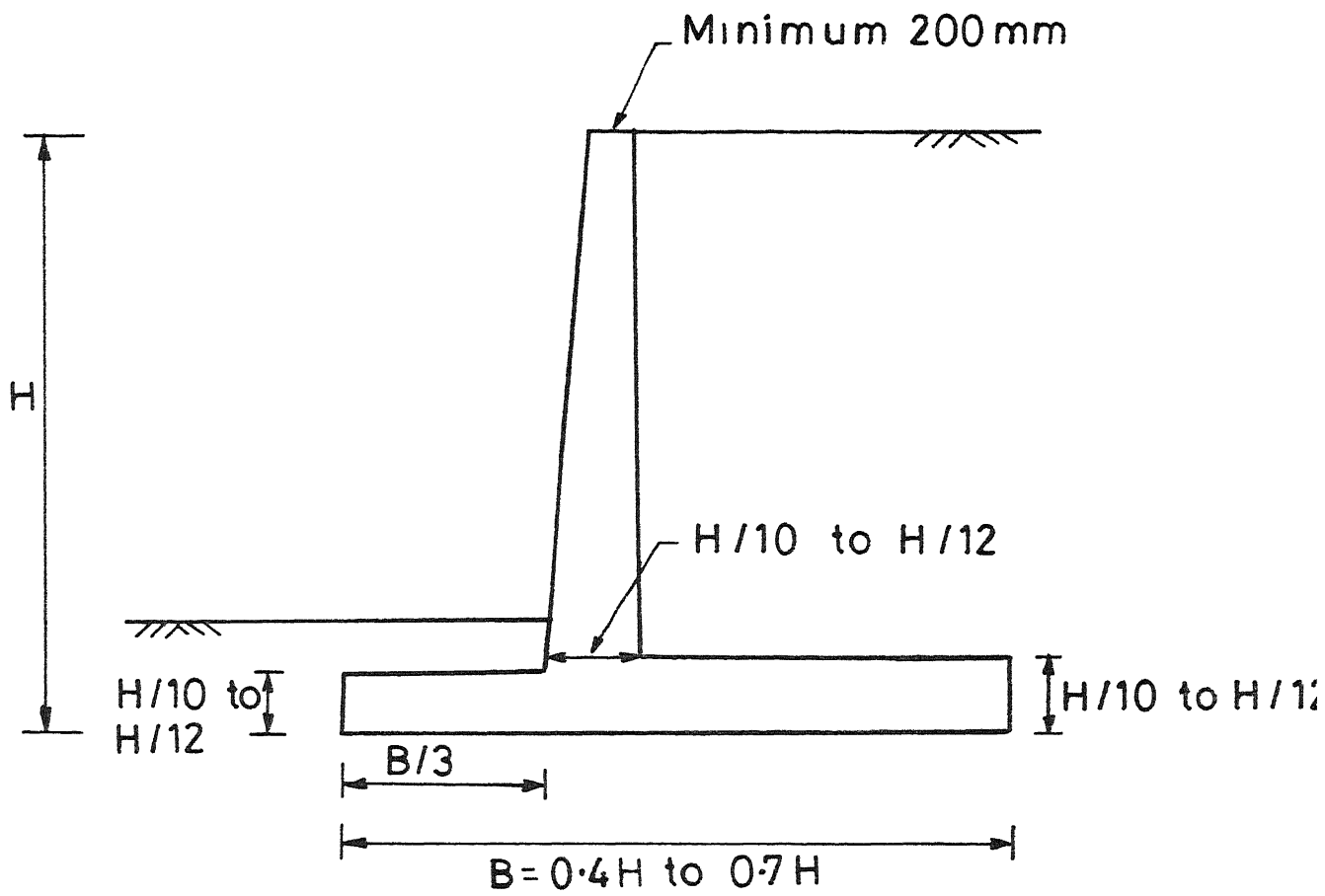


FIG. 4.4 : INITIAL FEASIBLE DESIGN

CHAPTER V

RESULTS, DISCUSSION AND CONCLUSIONS

5.1 General

The formulation described earlier is applied in seeking the minimum cost design of a free standing cantilever retaining wall on (i) rigid and (ii) flexible, foundations.

Four classes of cohesionless soils have been considered in the present work. The representative values of the properties of these soils are given in Table 5.1

Table 5.1: REPRESENTATIVE PROPERTIES OF SOIL

Soil	c N/m^2	ϕ Degrees	γ N/m^3	K_s $N/m^2 \cdot m$
Gravel	0.0	42.0	19620.0	125 10^6
Sand well graded	0.0	38.0	18640.0	80 10^6
Sand uniformly graded	0.0	34.0	18150.0	60 10^6
Non-Plastic Silt	0.0	28.0	17265.0	45 10^6

The above values have been taken from Bowles (1988), Huntington (1957) and Lambe & Whitman (1969). It is assumed that the backfill and the foundation materials are the same in a particular case. The overall height of the wall is varied from three to six meters. The foundation level is at a minimum of one

meter below ground level.

Concrete of grade M 15 and steel of grade FE 415 have been used. 12 mm diameter bars have been used for the heel and toe projections. For the stem, 16 mm diameter bars are used for wall heights up to 4.5 m and 20 mm diameter bars for wall heights above 4.5 m. The clear cover to the main steel is taken as 50 mm. The unit cost of concrete is taken to be Rs. 1100 per cubic meter while that of steel is Rs. 9500 per ton.

All computations have been carried out on the Hewlett Packard 9000 system. The CPU time taken to obtain an optimum design is about 5 seconds for retaining walls on rigid foundation and about 120 seconds for retaining walls on flexible foundation.

Results for each class of soil are presented below.

5.2 Soil: Gravel

Table 5.2 and Fig 5.1(a) show the variation of minimum cost with the height of the wall.

Table 5.2

Overall height of wall (m)	Minimum cost in Rupees/m	
	rigid fdn.	flexible fdn
3.0	1286	1256
3.5	1605	1571
4.0	2017	1967
4.5	2513	2435
5.0	3175	3069
5.5	3827	3688
6.0	4564	4374

The minimum cost design of the retaining wall on rigid foundation is slightly higher than the corresponding cost on flexible foundation for all heights considered.

For rigid foundation behavior, the active constraints are.

- (a) Limit on the eccentricity,
- (b) Moment of resistance at the stem base,
- (c) Shear resistance of the toe projection,
- (d) Moment of resistance of the heel projection

Constraints (a), (b) and (c) above, are active for all wall heights considered while constraint (d) is active for wall heights ranging from 3.0 m to 5.5 m. Thereafter, shear governs the design of the heel. An additional constraint, namely, lower bound on the stem base thickness, is active for wall heights up to 3.5 m only. The percentages of steel are seen to adjust in such a manner as to yield balanced sections.

The variation of the sizing variables, corresponding to the optimum design, with the height of the wall is shown in Fig.5.2. The stem base thickness (X_1), the depth of the toe projection (X_2) and the depth of the heel projection (X_5) are seen to increase as the height of the wall increases. The length of the heel projection (X_4) increases very rapidly with the wall height. This is because the weight of the soil above the heel is mainly responsible for the stability of the wall against sliding and overturning due to the lateral earth pressure. The length of the toe projection (X_3) is seen to increase as the wall height increases up to 4.0 m. Thereafter it decreases gradually.

For flexible foundation behavior, once again all constraints listed above, except constraint (a) which is non-existent, turn

out to be active. In addition, the constraint for safety against overturning is active for all wall heights.

Referring to Fig 5.2, as the wall height increases, the sizing variables, corresponding to the optimum design, show a trend similar to that obtained for a rigid foundation. The percentage difference in minimum cost of the optimum designs corresponding to a rigid foundation and a flexible one is seen to vary from 2.33 % to 4.15 % as the height of the wall increases from 3.0 m to 6.0 m. The thickness of the stem base is the same for both cases. The thickness and length of the toe projection is less for a flexible foundation for all wall heights considered. The length of the heel projection is also greater for wall heights up to 5.5 m. The thickness of the heel projection is greater for wall heights up to 4.5 m. The base width of the wall footing is about 7.36 % smaller for a flexible foundation.

The lower cost for optimum design for a flexible foundation is due to the fact that the soil is allowed to withstand limited tension. The latter is not admissible for a rigid foundation. The difference in the thickness of the heel and the toe projections obtained is due to the difference in the bearing pressure distribution under the footing. A typical variation of bearing pressure obtained for a flexible foundation is illustrated in Fig.5.3.

Gravels have a high angle of shearing resistance. Consequently, they offer high resistance to sliding, foundation bearing failure and slip circle failure. The allowable bearing capacity obtained from the expressions given in appendix A varies from 530 KN/m^2 to 670 KN/m^2 . The base width of the wall is seen to

reduce till either the eccentricity is maximum permissible for rigid foundation behavior or the safety against overturning is critical for flexible foundation behavior. Shear governs the toe projection design as it is small in length and is subjected to high foundation bearing pressures.

5.3 Soil: Well Graded Sand

Table 5.3 and Fig.5.1(b) show the variation of minimum cost with the height of the wall.

Table 5.3

Overall height of wall (m)	Minimum cost in Rupees/m	
	rigid fdn.	flexible fdn.
3 0	1325	1310
3 5	1679	1645
4 0	2134	2075
4 5	2668	2580
5.0	3378	3260
5 5	4084	3930
6 0	4878	4686

Retaining walls on rigid foundation have a minimum cost slightly higher than the corresponding cost on flexible foundation for all wall heights considered.

For rigid foundation behavior the active constraints are the same as for gravel in section 5.2. However, the constraint for the moment of resistance of the heel is active for the entire range of wall heights. The variation of the sizing variables, corresponding to the optimum design, with the height of the wall

is shown in Fig.5 4. The trend observed is the same as that for gravel.

For flexible foundation behavior, the active constraints are the same as for gravel in section 5.2. The sizing variables, corresponding to the optimum design, show a similar trend.

The percentage difference in minimum cost of the optimum designs varies from 1.13 % to 3.94 % as the height of the wall increases from 3 0 m to 6.0 m. The thickness of the stem is the same for both. The length and the thickness of the toe projection is less for flexible foundation behavior. The length of the heel projection is greater for wall heights up to 5 0 m. The thickness of the heel projection is greater for flexible foundation behavior for wall heights up to 4.0 m. The base width is smaller by 6 85 % for flexible foundation behavior.

The allowable bearing capacity obtained varies from 245 KN/m^2 to about 300 KN/m^2 . The similarity in behavior of well graded sand and gravel is because both have high angles of shearing resistance.

5.4 Soil: Uniformly Graded Sand

Table 5.4 and Fig.5.1(c) show the variation of minimum cost with the height of the wall.

Table 5.4

Overall height of wall (m)	Minimum cost in Rupees/m	
	rigid fdn.	flexible fdn
3.0	1373	1348
3.5	1769	1728
4.0	2270	2203
4.5	2853	2765
5.0	3654	3530
5.5	4457	4297
6.0	5379	5170

Retaining walls on flexible foundations give a lower minimum cost as compared to those on rigid foundations for all heights considered

For rigid foundation behavior the constraints for the moment of resistance of the stem and heel projection and the shear resistance of the toe, are active for all wall heights considered. The lower bound on the thickness of the stem base is active for wall heights up to 3.5 m only. The constraint for limit on the eccentricity is active for wall heights up to 4.5 m only. Thereafter, the constraint for maximum foundation bearing pressure is active. All the steel percentages adjust to yield balanced sections.

The variation of the sizing variables, corresponding to the optimum design, with the height of the wall is shown in Fig.5.5. The stem base thickness and the depth of the toe and heel

projections are seen to increase as the wall height increases from 3.0 m to 6.0 m. The length of the heel projection increases very rapidly with the wall height.

For flexible foundation behavior, all constraints mentioned above, excluding the limit on the eccentricity, are active. The constraint for safety against overturning is active for wall heights up to 4.0 m, beyond which, the constraint for maximum foundation bearing pressure becomes active. Referring to Fig 5.5, the sizing variables corresponding to the optimum design, show a trend similar to that observed for a rigid foundation.

The percentage difference in minimum cost of the optimum designs varies from 1.82 % to 3.89 % as the wall height increases from 3.0 m to 6.0 m. The stem thickness is the same for both. The thickness of the toe projection is less for flexible foundation behavior. The length of the toe projection is substantially less for wall heights up to 5.0 m. The length of the heel projection is greater for wall heights up to 4.5 m. Thereafter it is less. The base width of the wall is smaller by about 4.88 % for flexible foundation behavior.

The value of allowable bearing capacity obtained varies from 124 KN/m^2 to 156 KN/m^2 . Hence, for a height of about 4.0 m to 4.5 m, the constraint for maximum foundation bearing pressure becomes active as the base width is small and the vertical load on the foundation is large leading to high bearing pressure.

5.5 Soil: Non-plastic silt

Table 5.5 and Fig.5 1(d) show the variation of minimum cost with the height of the wall

Table 5.5

Overall height of wall (m)	Minimum cost in Rupees / m	
	rigid fdn.	flexible fdn.
3.0	1556	1490
3.5	2080	1994
4.0	2704	2598
4.5	3536	3398
5.0	4570	4439
5.5	5765	5641
6.0	6997	7106

The wall on a flexible foundation gives a lower minimum cost as compared to the wall on a rigid foundation. However, this is observed for wall heights ranging from 3.0 m to 5.5 m only. For a wall height of 6.0 m the former has a higher minimum cost.

For rigid foundation behavior, the constraints for moment of resistance of the stem, heel and toe, are active for all wall heights. The constraint for maximum foundation bearing pressure is active for wall heights from 3.0 m to 4.5 m only. For wall heights of 5.0 m and above, the constraints for safety against sliding and slip circle failure are active. The percentages of steel adjust to yield balanced sections. The lower bound on the stem base thickness is active for wall height of 3.0 m only.

The variation of the sizing variables, corresponding to the optimum design, with the height of the wall shown in Fig 5.6. The

thickness of the stem base and the depth of the toe and heel projections are seen to increase with the wall height. The length of the toe projection increases gradually with an increase in wall height up to 4.5 m. Thereafter, a sharp increase is noticed up to a wall height of 6.0 m. The length of the heel projection increases with wall height up to 4.5 m. Then a decrease is noticed till a wall height of 5.0 m. Thereafter a gradual increase takes place. This behavior is due to the fact that at a wall height of 4.5 m the constraint for slip circle failure becomes active while that for maximum foundation bearing pressure ceases to be active. The base width needs to be increased to maintain stability of the wall. Increase in the length of the toe projection results in an increase in the factor of safety against slip circle failure. Increase in the length of the heel projection will also result in an increase in the factor of safety, though at a much slower rate. Hence, the length of the toe projection is seen to increase in order to maintain stability.

For flexible foundation behavior, the constraints for moment of resistance of the stem and heel and the constraint for maximum foundation bearing pressure are active for all wall heights considered. The constraint for moment of resistance of the toe is active from a wall height of 3.0 m to 5.5 m only. Thereafter, shear governs the toe design. The constraint for safety against slip circle failure is active for a wall height of 4.5 m and 5.0 m only. The constraint for lower bound on the stem base width is active for a wall height of 3.0 m only. The percentages of steel adjust to yield balanced sections. Referring to Fig 5.6, the sizing variables corresponding to the optimum design, show a trend

similar to that observed for a rigid foundation.

The percentage difference in minimum cost of the optimum designs is seen to decrease from 4.25 % to 2.5 % as the wall height increases from 3.0 m to 5.5 m. For a wall height of 6.0 m the wall on a rigid foundation has a cost lower by about 1.2 % with respect to the corresponding cost for a wall on a flexible foundation. The stem thickness is the same for both. The thickness of the toe projection is less for flexible foundation. The length of the toe projection is less for wall heights up to 4.5 m. Thereafter, it is almost same for both cases. The length of the heel projection is greater for wall heights exceeding 4.5 m.

Non-plastic silts have a low angle of shearing resistance. Hence, a large base width is required to maintain stability against foundation bearing failure, slip circle failure and sliding failure. The allowable bearing capacity obtained varies from 54 KN/m^2 to 99 KN/m^2 . As this value is low, the constraint for maximum foundation bearing pressure is seen to be active for all wall heights considered.

5.6 Some Salient Observations

Referring to Fig 5.1, it is observed that the minimum cost of the wall increases as the soil changes from gravel to well graded sand to uniformly graded sand and finally non-plastic silt. This is due to the fact that shearing resistance of the soil reduces in that order. A lower angle of shearing resistance results in a higher lateral earth pressure being exerted on the wall. This results in a higher minimum cost.

It is interesting to note that even though in the flexible

foundation behavior the soil has been allowed to withstand limited tension, no tension occurs in the foundation for all classes of soil corresponding to the optimum design

5.7 Guidelines for Preliminary Optimum Design

A study of the optimum designs for each class of soil indicates that the following proportioning of the sizing variables will yield a near optimum design.

Table 5.6: SIZING VARIABLES FOR NEAR OPTIMUM DESIGN

Variable	Soil			
	Gravel	Well Graded Sand	Uniformly Graded Sand	Non-plastic Silt
X_1	$H_w/13$	$H_w/12$	$H_w/11$	$H_w/10 - H_w/11$
X_2	$H_w/16$	$H_w/15$	$H_w/14$	$H_w/15 - H_w/12$
X_3	$H_w/6 - H_w/10$	$H_w/8$	$H_w/5 - H_w/8$	$H_w/3 - H_w/2$
X_4	$H_w/6 - H_w/4$	$H_w/6 - H_w/4$	$H_w/5 - H_w/4$	$H_w/3.5 - H_w/4$
X_5	$H_w/16 - H_w/15$	$H_w/15$	$H_w/14$	$H_w/16 - H_w/18$

The different cross sections need to be designed as balanced sections for minimum cost.

5.7 Conclusions

- (1) The minimum cost design of the retaining wall on rigid foundation is seen to be slightly higher than the corresponding cost on flexible foundation for all wall heights ranging from 3.0 m to 6.0 m.
- (ii) There is no significant reduction in minimum cost corresponding to the optimum design of retaining walls considered on flexible foundations.
- (iii) The optimum design is a fully stressed design as each component is a balanced section. This would have been expected as the system is determinate when the wall is on a rigid foundation. However, it also turns out to be so when the wall is considered on a flexible foundation even though this system is indeterminate. The reason for this is the fact that the flexibility of the foundation has very little effect on the optimum design of the retaining wall.
- (iv) The soil does not experience any tension effects for the flexible foundation.
- (v) Optimum design of retaining walls of the heights considered, can be carried out by assuming that the foundation is rigid.

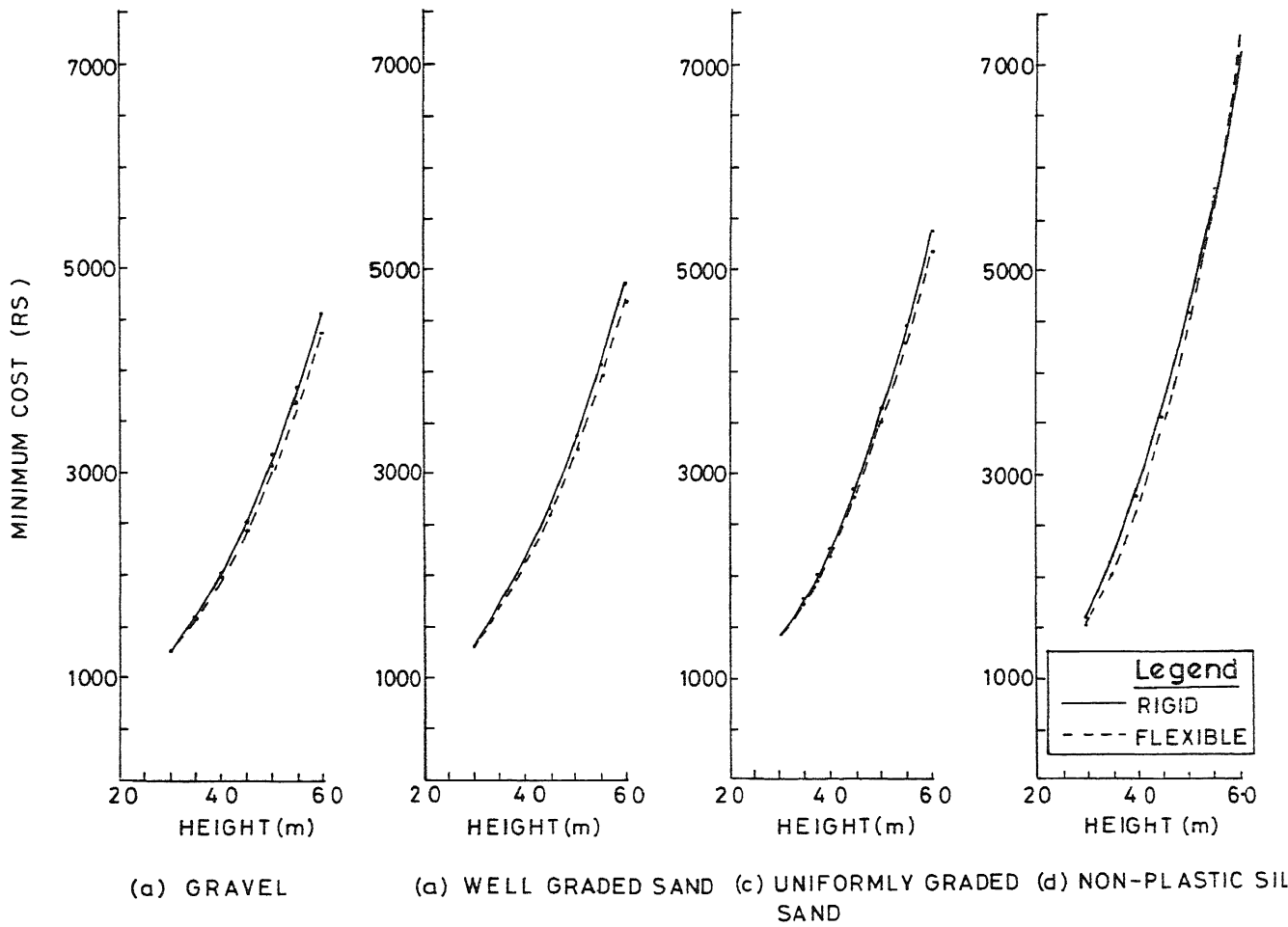


FIG 5.1 VARIATION OF MINIMUM COST W R T HEIGHT OF WALL

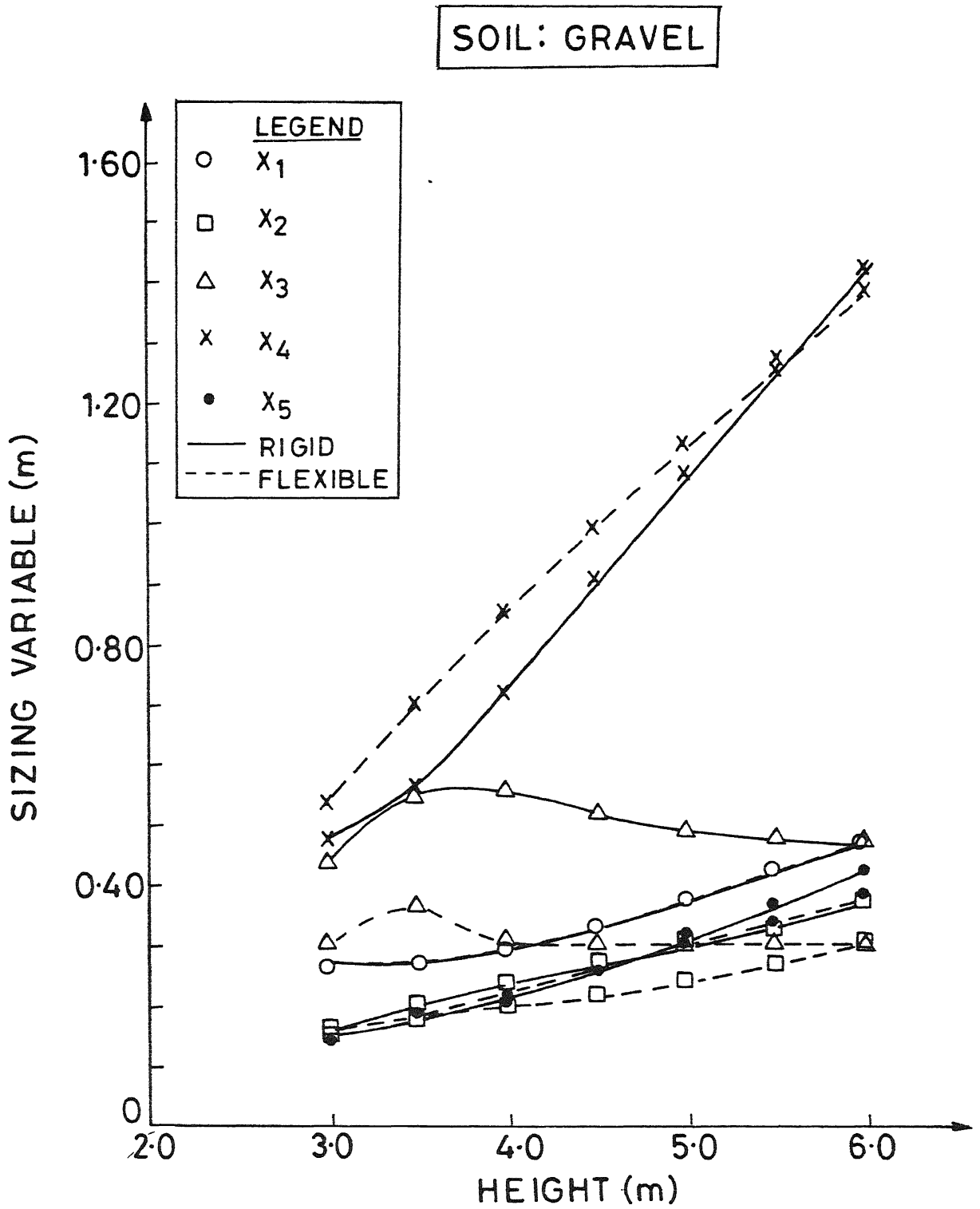


FIG 5.2: VARIATION OF SIZING VARIABLES WITH HEIGHT

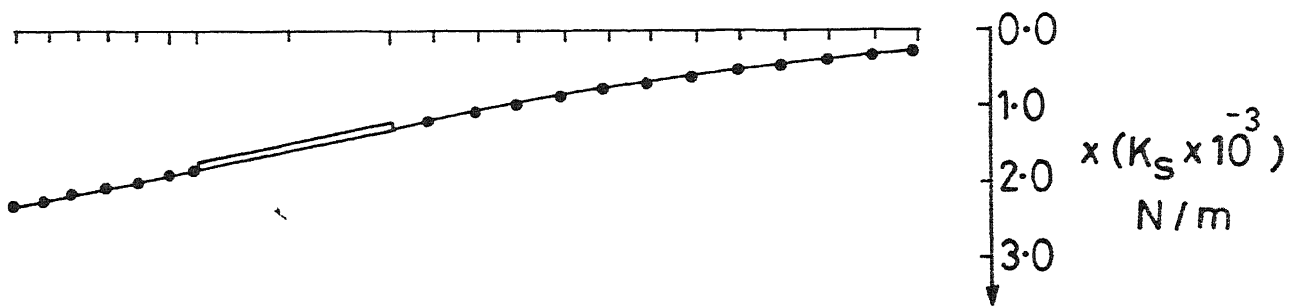


FIG. 5.3: TYPICAL VARIATION OF BEARING PRESSURE
FOR FLEXIBLE FOUNDATION

SOIL: WELL GRADED SAND

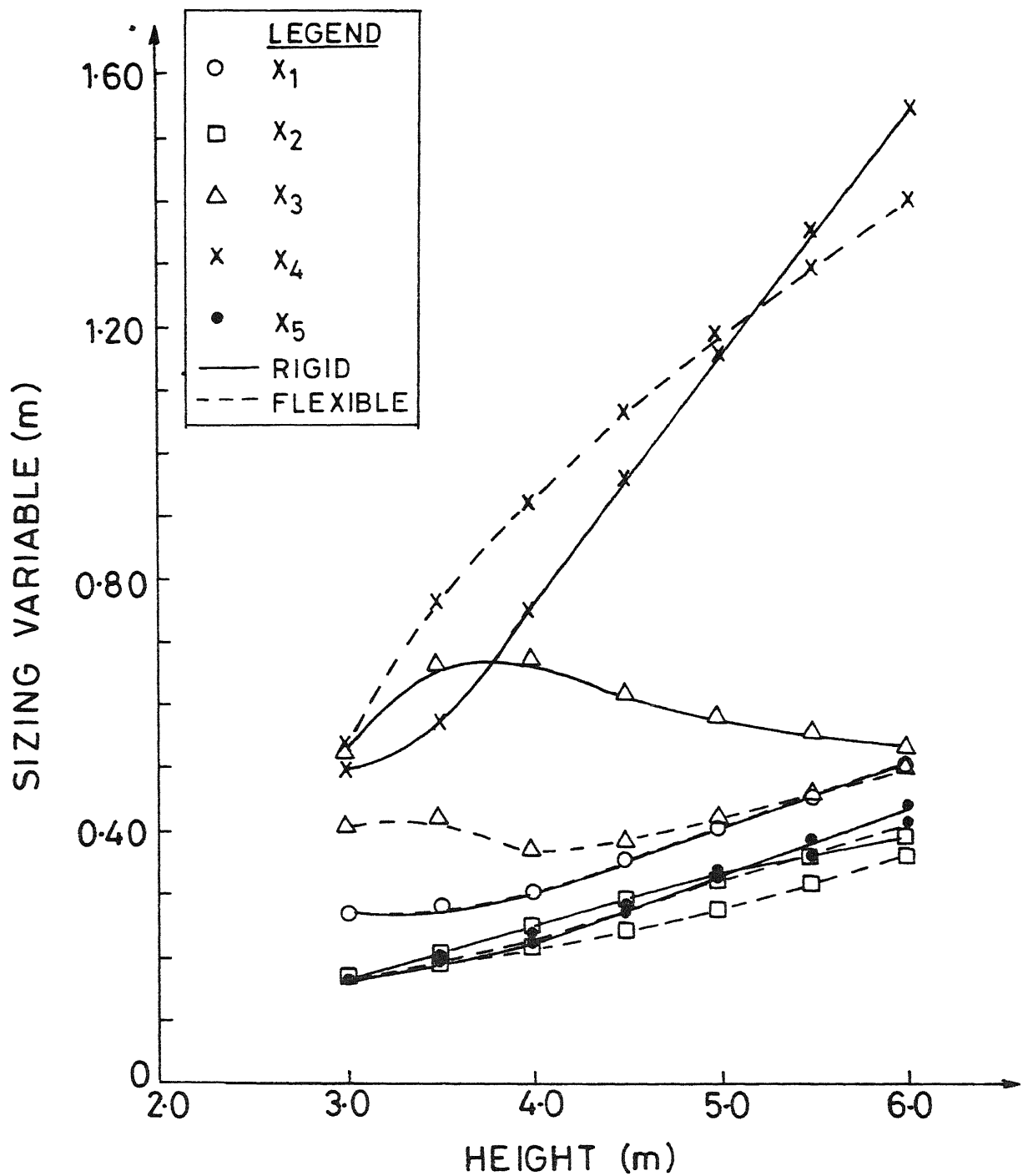


FIG.5.4: VARIATION OF SIZING VARIABLES WITH HEIGHT

SOIL: UNIFORMLY GRADED SAND

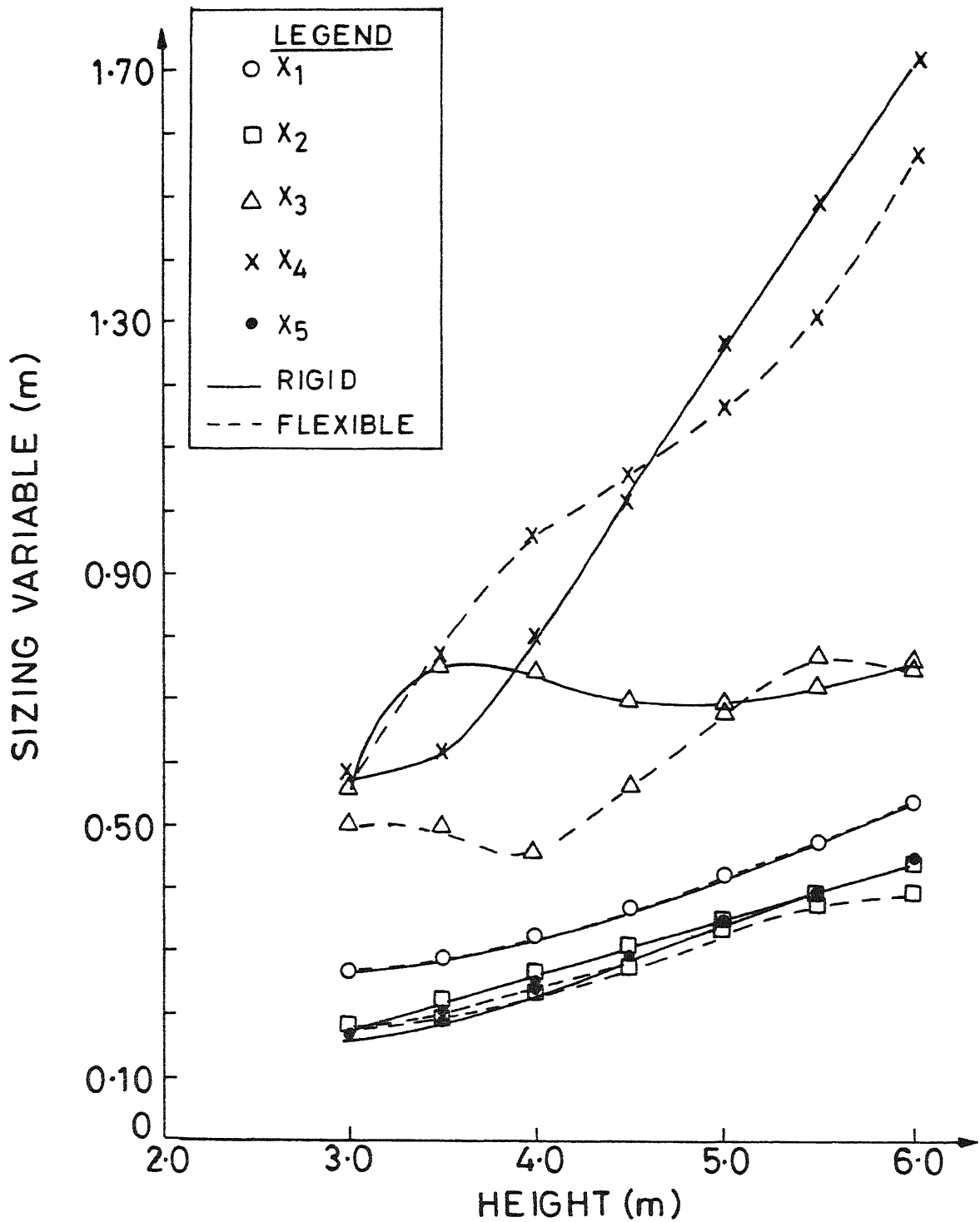


FIG 55: VARIATION OF SIZING VARIABLES WITH HEIGHT

SOIL : NON-PLASTIC SILT

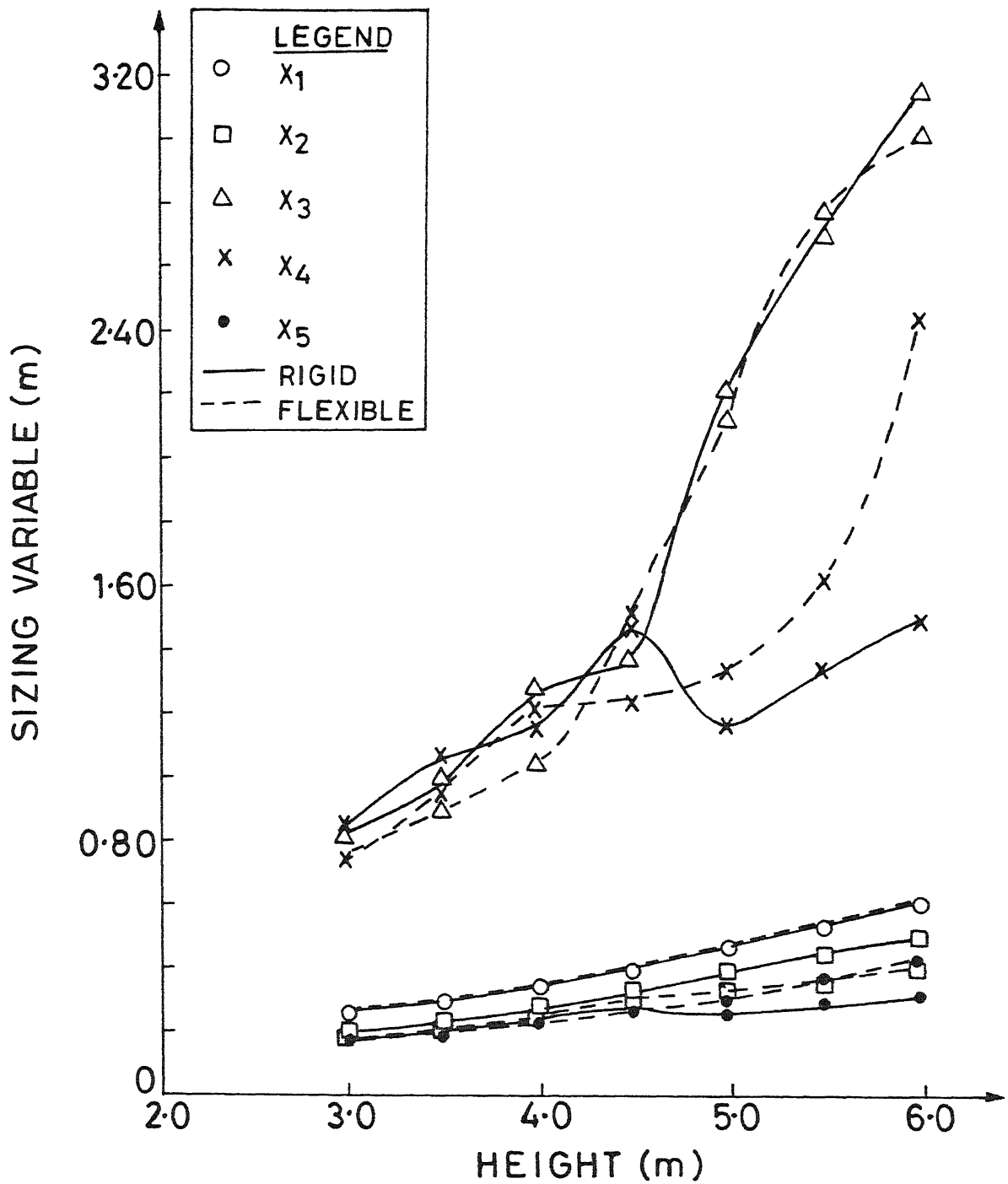


FIG 5.6: VARIATION OF SIZING VARIABLES WITH HEIGHT

LIST OF REFERENCES

- 1 American Concrete Institute (1983). Building Code Requirements for Reinforced Concrete (ACI 318-83), ACI, Detroit, Mich
2. Arora, J. S. (1989). Introduction to Optimum Design, McGraw - Hill Book Co., New York
3. Bowles, J. E (1988): Foundation Analysis and Design, 4/e, McGraw-Hill Book Co , New York.
- 4 Bowles, J E (1974): Analytical and Computer Methods in Foundation Engineering, McGraw-Hill Book Co., New York.
- 5 Dayaratnam, P. (1983) Reinforced Concrete Structures, Oxford IBH Publishing Co , New Delhi
- 6 Ferguson, P. M., J. E Breen and J O. Jirsa (1988) Reinforced Concrete Fundamentals, 5/e, John Wiley and Sons, Inc., New York
- 7 Fiacco, A. V and G P McCormick (1964). Computational Algorithm for the Sequential Unconstrained Minimization Technique for Nonlinear Programming, Management Science, vol. 10, no. 4.
8. Fox, R. L. (1971) Optimization Methods for Engineering Design, Addison-Wesley Publishing Co , Reading, Ma.
- 9 Hetenyi, M. (1946) Beams on Elastic Foundations, The Univ. of Michigan Press, Ann Arbor, Mich.
- 10 Huntington, W. C (1957) Earth Pressure and Retaining Walls, John Wiley and Sons, Inc., New York
11. IS 456 (1978): Code of Practice for Plain and Reinforced Concrete, Indian Standards Institution, New Delhi.
- 12 Keskar, A V (1979): Optimal Design of Thin and Thick Walled Civil Engineering Structures, Phd Thesis, Dept of Civil Engineering, I I.T., Kanpur.
13. Lambe, T. W. and R V. Whitman (1969) Soil Mechanics, John Wiley and Sons, Inc , New York.
14. Mallick, S. K. and A. P. Gupta (1989). Reinforced Concrete, 5/e, Oxford IBH Publishing Co , New Delhi.
15. Meyerhof, G. G. (1963) " Some Recent Research on the Bearing Capacity of Foundations," Can Geotech. Journal, Ottawa, vol. 1, no 1, Sept., pp 16-26

16. Rao, S. S. (1984): Optimization, Theory and Applications, Wiley Eastern Ltd, New Delhi.
17. Reddy, J. N. (1985) An Introduction to the Finite Element Method, McGraw-Hill Book Co, New York.
18. Selvadurai, A. P. S. (1979): Elastic Analysis of Soil-Foundation Interaction, Elsevier, Amsterdam.
19. Teng, W. C. (1962) Foundation Design, Prentice Hall of India Pvt. Ltd, New Delhi
20. Terzaghi, K. and R. B. Peck (1967): Soil Mechanics in Engineering Practice, John Wiley and Sons, Inc, New York.
21. Vanderplaats, G. N. (1984): Numerical Optimization Techniques for Engineering Design, McGraw-Hill Book Co, New York
22. Wang, C. K. (1983). Intermediate Structural Analysis, McGraw-Hill Book Co., New York
23. Wang, C. K. (1970) Matrix Methods of Structural Analysis, 2/e, Intext Educational Publishers, Scranton, Pa
24. Wellington, Office of the Chief Design Engineer (Civil) (1973): Retaining Wall Design Notes, New Zealand
25. Zienkiewicz, O. C. (1979) The Finite Element Method, 3/e, Tata McGraw-Hill Publishing Co Ltd., New Delhi.

APPENDIX A

MEYERHOF'S BEARING CAPACITY EQUATIONS

Meyerhof (1963) proposed the following equation to estimate the bearing capacity of a strip footing subjected to an eccentric loading.

$$Q_{ult} = c N_c d_c i_c + \bar{q} N_q d_q i_q + 0.5 \gamma B' N_\gamma d_\gamma i_\gamma \quad (A.1)$$

where Q_{ult} is the ultimate bearing capacity.

The factors N_c , N_q and N_γ are given by the expressions,

$$N_q = e^{\pi \tan \phi} \tan^2(45 + \phi/2)$$

$$N_c = (N_q - 1) \cot \phi$$

$$N_\gamma = (N_q - 1) \tan(1.4\phi) \quad (A.2)$$

The depth factors d_c , d_q and d_γ are given by

$$d_c = 1 + 0.2 \sqrt{K'_p} \frac{D}{B} \quad \text{for any value of } \phi$$

$$d_q = d_\gamma = 1 + 0.1 \sqrt{K'_p} \frac{D}{B} \quad \text{for } \phi > 10 \quad (A.3)$$

The inclination factors i_c , i_q and i_γ are given by

$$i_c = i_q = (1 - \theta^\circ / 90^\circ)^2 \quad \text{for any } \phi$$

$$i_\gamma = (1 - \theta^\circ / \phi^\circ)^2 \quad \text{for } \phi > 0 \quad (A.4)$$

In the above expressions,

$B' = B - 2e$; is the effective breadth of the footing,

B is the breadth of the footing,

e is the eccentricity of the resultant load on the

foundation,

D is the depth of the footing below ground surface,

θ is the angle of the resultant measured from vertical without a sign,

c and ϕ are as defined before,

$$K'_p = \tan^2(45 + \phi/2)$$

A factor of safety of 3.0 is applied to the estimated ultimate bearing capacity to yield the allowable bearing capacity.

APPENDIX B

COMPUTATION OF FACTOR OF SAFETY FOR SLIP CIRCLE FAILURE

This type of failure is illustrated in Fig.3.2. It usually occurs along a curved surface, which is assumed to be cylindrical and which passes through the heel of the retaining wall

The force that causes sliding along the arc is denoted by ΣT . The resisting force is the shear strength of the soil along the arc, denoted by S . The factor of safety is given by

$$F_s = \frac{S}{\Sigma T} = \frac{\Sigma \sigma_n \tan \phi + cl}{\Sigma T} \quad (B.1)$$

where l is the length of the arc,

σ_n is the unit normal stress along the arc,

c and ϕ are as defined before

Due to the varying direction of σ_n , $\Sigma \sigma_n$ does not equal N , the resultant normal force on the arc. The force ΣT can be determined easily by considering moment equilibrium about the assumed arc center O in Fig 3.2. However, the computations required to determine $\Sigma \sigma_n$ are more complex. Hence, Huntington (1957) suggests a simple approximate method that yields values within 5% of the true value of the factor of safety.

The portion AD of the trial arc in Fig 3.2 is assumed to coincide with the Rankine's inner failure plane so that the force acting against the virtual back of the wall is the active earth pressure, P_a . Let ΣV and ΣH be the vertical and horizontal components of the resultant pressure on the foundation of the

retaining wall. Let the weight of the volume of the soil in the area Aabc in Fig.B 1 be denoted by W'_a . Define

$$\Sigma V_1 = \Sigma V - W'_a$$

Let the resultant R_1 of ΣH and ΣV_1 , intersect the trial arc at point O_1 in Fig B.1(a). Let N_1 and T_1 be the normal and tangential components of R_1 at point O_1 . The weight of soil in area Aade including the weight of soil displaced by concrete, is,

$$W_2 = 2 \gamma h_2 x_0 \quad (B.2)$$

The sum of the normal components along the arc, due to W_2 , is,

$$N_2 = g_2 W_2 \quad (B.3)$$

Due to symmetry, the tangential component, T_2 , is equal to zero. The area of the segment AO_1e in Fig. B.1(a), may be assumed to be equal to two - thirds of the area of the circumscribing rectangle. Thus, the weight is,

$$W_3 = 1.33 \gamma h_3 x_0 \quad (B.4)$$

$$N_3 = g_3 W_3 \quad (B.5)$$

Due to symmetry, $T_3 = 0$

The coefficients, g_2 and g_3 , can be assumed as equal to 0.95 for values of θ up to 45° without introducing significant errors. The weight of soil in the area dec, which may be assumed as triangular, is,

$$W_4 = 0.5 \gamma h_2 x' \quad (B.6)$$

Let N_4 and T_4 be the normal and tangential components of W_4 . T_4 is negative as it opposes the action of T_1 .

The factor of safety can be computed from (B.1) with

$$\begin{aligned} \Sigma N &= N_1 + N_2 + N_3 + N_4, \\ \Sigma T &= T_1 - T_4 \end{aligned} \quad (B.7)$$

A number of trial arc centers are to be assumed and the critical arc center which yields the minimum factor of safety is to be found. However, Huntington suggests that the point O in Fig B.1 may be assumed as a reasonably good arc center for cohesionless soil and with no surcharge on the backfill.

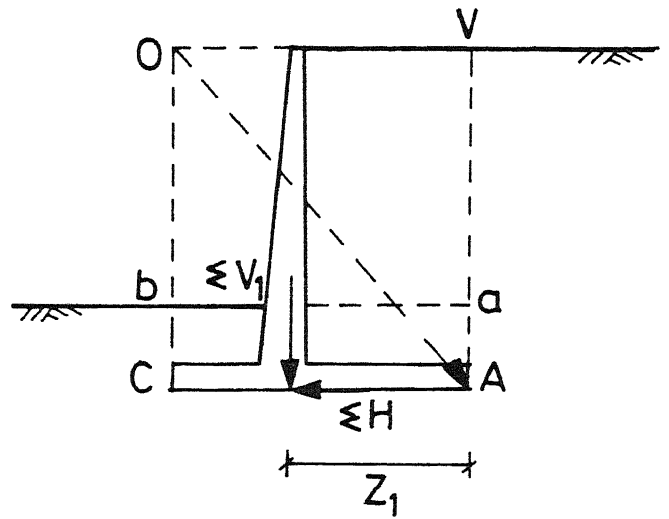


Fig. B-1

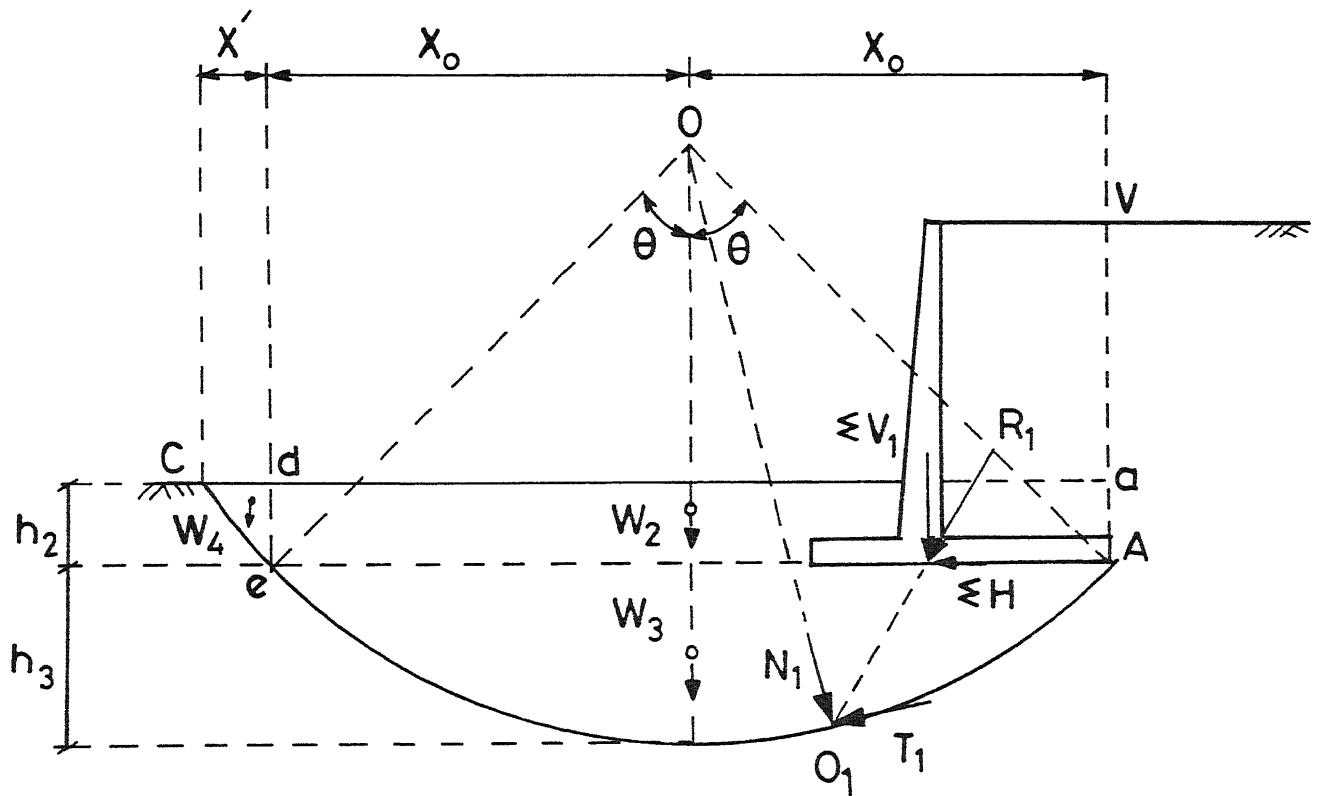


Fig B-1(a)

FIG. B-1: FACTOR OF SAFETY FOR SLIP CIRCLE FAILURE

1.100 .

10-M-ME D-CPT